



**NAVAL
POSTGRADUATE
SCHOOL**

MONTEREY, CALIFORNIA

THESIS

**ANALYSIS OF AUTONOMOUS LOAD FOLLOWING
(ALF) IN ADVANCED FAST REACTORS**

by

Brad W. Kinnamon

December 2018

Thesis Advisor:

Craig F. Smith

Second Reader:

Raymond M. Gamache

Approved for public release. Distribution is unlimited.

THIS PAGE INTENTIONALLY LEFT BLANK

REPORT DOCUMENTATION PAGE			Form Approved OMB No. 0704-0188	
Public reporting burden for this collection of information is estimated to average 1 hour per response, including the time for reviewing instruction, searching existing data sources, gathering and maintaining the data needed, and completing and reviewing the collection of information. Send comments regarding this burden estimate or any other aspect of this collection of information, including suggestions for reducing this burden, to Washington headquarters Services, Directorate for Information Operations and Reports, 1215 Jefferson Davis Highway, Suite 1204, Arlington, VA 22202-4302, and to the Office of Management and Budget, Paperwork Reduction Project (0704-0188) Washington, DC 20503.				
1. AGENCY USE ONLY (Leave blank)		2. REPORT DATE December 2018	3. REPORT TYPE AND DATES COVERED Master's thesis	
4. TITLE AND SUBTITLE ANALYSIS OF AUTONOMOUS LOAD FOLLOWING (ALF) IN ADVANCED FAST REACTORS			5. FUNDING NUMBERS GEN IV Fast Reactors	
6. AUTHOR(S) Brad W. Kinnamon				
7. PERFORMING ORGANIZATION NAME(S) AND ADDRESS(ES) Naval Postgraduate School Monterey, CA 93943-5000			8. PERFORMING ORGANIZATION REPORT NUMBER	
9. SPONSORING / MONITORING AGENCY NAME(S) AND ADDRESS(ES) DTRA			10. SPONSORING / MONITORING AGENCY REPORT NUMBER	
11. SUPPLEMENTARY NOTES The views expressed in this thesis are those of the author and do not reflect the official policy or position of the Department of Defense or the U.S. Government.				
12a. DISTRIBUTION / AVAILABILITY STATEMENT Approved for public release. Distribution is unlimited.			12b. DISTRIBUTION CODE A	
13. ABSTRACT (maximum 200 words) <p>The autonomous load following (ALF) properties of fast-spectrum nuclear reactors offer great potential for increased electric grid stability, reduction in control rod mechanism wear, and less operator action for small power transients experienced on a daily basis. These features can result in design simplification and enhanced safety of such reactor systems. Thermal-hydraulic transients result in reactivity feedback from the coolant to curb power transients and return the reactor to a stable, critical condition. The speed of the reactivity feedback and the resulting limits on how large a transient can be controlled through autonomous load following are based to a great extent on the intrinsic properties of the coolant and its effects on the associated reactor kinetics. Lead, lead bismuth eutectic (LBE), and sodium are coolants that have properties amenable to ALF, and these primary coolant types are among the promising options for advanced fast reactors under the Generation IV program. This paper reviews the relevant properties of each coolant type and presents the heat-transfer modeling results of analyses using evaluated nuclear data files (ENDF) data and MATLAB to simulate their respective reactivity responses for a simplified fast reactor design. The results provide insight into comparison of coolant types based on reactivity feedback and autonomous load following capability in future fast reactor designs.</p>				
14. SUBJECT TERMS nuclear, reactor, lead, sodium, lead bismuth, fast spectrum, autonomous load following			15. NUMBER OF PAGES 73	
			16. PRICE CODE	
17. SECURITY CLASSIFICATION OF REPORT Unclassified	18. SECURITY CLASSIFICATION OF THIS PAGE Unclassified	19. SECURITY CLASSIFICATION OF ABSTRACT Unclassified	20. LIMITATION OF ABSTRACT UU	

THIS PAGE INTENTIONALLY LEFT BLANK

Approved for public release. Distribution is unlimited.

**ANALYSIS OF AUTONOMOUS LOAD FOLLOWING (ALF) IN ADVANCED
FAST REACTORS**

Brad W. Kinnamon
Lieutenant Commander, United States Navy

Submitted in partial fulfillment of the
requirements for the degree of

MASTER OF SCIENCE IN PHYSICS

from the

**NAVAL POSTGRADUATE SCHOOL
December 2018**

Approved by: Craig F. Smith
Advisor

Raymond M. Gamache
Second Reader

Kevin B. Smith
Chair, Department of Physics

THIS PAGE INTENTIONALLY LEFT BLANK

ABSTRACT

The autonomous load following (ALF) properties of fast-spectrum nuclear reactors offer great potential for increased electric grid stability, reduction in control rod mechanism wear, and less operator action for small power transients experienced on a daily basis. These features can result in design simplification and enhanced safety of such reactor systems. Thermal-hydraulic transients result in reactivity feedback from the coolant to curb power transients and return the reactor to a stable, critical condition. The speed of the reactivity feedback and the resulting limits on how large a transient can be controlled through autonomous load following are based to a great extent on the intrinsic properties of the coolant and its effects on the associated reactor kinetics. Lead, lead bismuth eutectic (LBE), and sodium are coolants that have properties amenable to ALF, and these primary coolant types are among the promising options for advanced fast reactors under the Generation IV program. This paper reviews the relevant properties of each coolant type and presents the heat-transfer modeling results of analyses using evaluated nuclear data files (ENDF) data and MATLAB to simulate their respective reactivity responses for a simplified fast reactor design. The results provide insight into comparison of coolant types based on reactivity feedback and autonomous load following capability in future fast reactor designs.

THIS PAGE INTENTIONALLY LEFT BLANK

TABLE OF CONTENTS

I.	INTRODUCTION.....	1
II.	PHYSICS OF FAST REACTOR LOAD FOLLOWING	5
A.	REACTOR COMPONENT BASICS.....	5
B.	NEUTRON INTERACTIONS.....	6
1.	Elastic Scattering	7
2.	Inelastic Scattering.....	7
3.	Radiative Capture.....	8
4.	Fission.....	8
C.	REACTOR FISSION PROCESS	8
D.	THERMAL VS. FAST REACTORS	9
E.	CRITICALITY AND REACTIVITY FEEDBACK.....	12
F.	REACTOR CONTROL AND LOAD FOLLOWING.....	16
III.	PROPERTIES OF COOLANTS	19
A.	PHYSICAL PROPERTIES	19
1.	Melting and Boiling Points.....	20
2.	Density.....	21
3.	Thermal Conductivity	22
4.	Specific Heat Capacity.....	24
5.	Viscosity	26
6.	Physical Properties Summary.....	27
B.	LIQUID METAL COOLANT NEUTRON INTERACTION PROPERTIES.....	28
1.	Neutron Interaction Summary by Coolant.....	28
2.	Radiative Capture Comparison.....	30
3.	Elastic Scattering Comparison	31
4.	Inelastic Scattering Comparison	32
IV.	PROCEDURE AND RESULTS	35
A.	DATA GATHERING	35
B.	MODELING EQUATIONS.....	38
C.	MATLAB RESULTS.....	42
D.	ANALYSIS	48
1.	Interpretations of dT/dt Graphs.....	48
2.	Reactivity Considerations	49

V. SUMMARY	51
LIST OF REFERENCES.....	53
INITIAL DISTRIBUTION LIST	55

LIST OF FIGURES

Figure 1.	Neutron Cross Sections for U-235. Adapted from [8].	11
Figure 2.	Neutron Cross Sections for U-238. Adapted from [8].	11
Figure 3.	Reactor Power and Reactivity vs. Time for Different Reactivity Coefficients. Adapted from [12].	15
Figure 4.	Temperature Effects on Density of Coolants. Adapted from [7].	22
Figure 5.	Temperature Effects on Thermal Conductivity of Coolants. Adapted from [7].	23
Figure 6.	Temperature Effects on Specific Heat Capacity of Coolants. Adapted from [7].	25
Figure 7.	Temperature Effects on Viscosity of Coolants. Adapted from [7].	26
Figure 8.	Desired Regions for Liquid Metal Coolant Physical Properties	27
Figure 9.	Neutron Interaction Cross Sections for Sodium – 23. Adapted from [8].	29
Figure 10.	Neutron Interaction Cross Sections for Lead – 208. Adapted from [8].	29
Figure 11.	Neutron Interaction Cross Sections for Bismuth – 209. Adapted from [8].	30
Figure 12.	Radiative Capture Cross Sections of Coolants. Adapted from [8].	31
Figure 13.	Elastic Scattering Cross Sections of Coolants. Adapted from [8].	32
Figure 14.	Inelastic Scattering Cross Sections for Coolants. Adapted from [8].	33
Figure 15.	Change in Reactivity for LBE-Cooled Reactor Based on Density Change. Source [20].	37
Figure 16.	Core Structure, Geometry, and Nodes for the Plant Dynamics Code. Source [18].	39
Figure 17.	Nodes for Core Temperatures. Source [18].	39
Figure 18.	Temperature Change Rate for Three Coolants for ARC-100 Design.	42

Figure 19.	Zoomed Temperature Change Rate for Three Coolants for ARC-100 Design.	43
Figure 20.	Temperature Change Rate for Three Coolants for STAR-LM Design.....	44
Figure 21.	Zoomed Temperature Change Rate for Three Coolants for STAR-LM Design.	44
Figure 22.	Temperature Change Rate for Three Coolants for SVBR-75 Design.....	45
Figure 23.	Zoomed Temperature Change Rate for Three Coolants for SVBR-75 Design.	45
Figure 24.	Change in Temperature Rate vs. Temperature for Three Reactor Designs.....	46
Figure 25.	Shifted Elastic Scattering Cross Sections of Coolants. Adapted from [8].....	47
Figure 26.	Shifted vs. Original Elastic Scattering Cross Sections of Coolants. Adapted from [8].....	48

LIST OF TABLES

Table 1.	Criticality Definitions and Graphs. Source [13].	13
Table 2.	Thermophysical Properties of Liquid Metals. Adapted from [7].	19
Table 3.	Temperature Dependent Coolant Reactivities	36
Table 4.	Atomic Density of Coolants.....	46

THIS PAGE INTENTIONALLY LEFT BLANK

LIST OF ACRONYMS AND ABBREVIATIONS

ARC	advanced reactor concepts
ALF	autonomous load following
BOL	beginning of life
EL	elastic scattering
ENDF	evaluated nuclear data files
eV	electron volt
GEN IV	Generation IV International Forum
GFR	gas cooled reactor
HTC	heat transfer coefficient
IFR	integral fast reactor
LBE	lead bismuth eutectic
LFR	lead cooled fast reactor
LWR	light water reactor
MeV	mega electron volt
MSR	molten salt reactor
NNPP	Naval Nuclear Propulsion Program
NON	inelastic scattering
peV	pico electron volt
PWR	pressurized water reactors
RC	radiative capture
SCWR	super critical water reactor
SVBR	lead bismuth fast reactor (Russian abbreviation)
SFR	sodium cooled fast reactor
VHTR	very high temperature reactor

THIS PAGE INTENTIONALLY LEFT BLANK

ACKNOWLEDGMENTS

I would like to thank several people for their help in completing this thesis:

Dr. Ray Gamache, for his reviews and suggestions in making nuclear power understandable to all readers.

Dr. Craig Smith, for being a patient advisor as we navigated many options for the scope of this thesis.

Zoe and Juniper, for being all smiles at the end of the day.

Kat Kinnamon, for being a loving wife and enduring many days and evenings of solo parenting as I researched, wrote, and revised this thesis.

THIS PAGE INTENTIONALLY LEFT BLANK

I. INTRODUCTION

As nuclear technology and research has advanced into the 21st century, a push is being made to move past the use of the current light water reactors (LWR) of the Generation II/III era into the advanced reactors of Generation IV [1]. These “GEN IV” reactors incorporate a varied combination of features including neutron spectrum (i.e., thermal vs. fast), moderators (i.e., water, graphite, or none), coolants (i.e., water, sodium, lead, or gas), and fuel types (i.e., oxides, metals, nitrides, or carbides) [1]. The combinations are generally grouped into six categories in the GEN IV hierarchy: sodium cooled fast reactor (SFR), lead cooled fast reactor (LFR), gas fast reactor (GFR), very high temperature reactor (VHTR), super critical water reactor (SCWR), and molten salt reactor (MSR) [1]. The LFR designs include pure lead coolant and lead-bismuth eutectic (LBE) coolant variations.

There are almost 450 land based and 180 ship and submarine born reactors currently in operation around the world, of which only a small fraction operating now or in the past have been non-water-cooled reactors [2]. This makes the push towards “different” reactors a slow and difficult process because the technology and designs for LWRs have been established, tested, and safely operated (with the exception of notable accidents at Three Mile Island, Chernobyl, and Fukushima Daiichi) for the past 70 years within the commercial industry and naval nuclear propulsion. Adding to international concern is that there have been several incidents related to naval nuclear propulsion, exclusively limited to Soviet/Russian submarines, several of which were liquid metal cooled. On the contrary, there have been no severe nuclear accidents within the United States naval nuclear propulsion program (NNPP), which has led to significant confidence in its current reactor designs. The successful history of water-cooled civilian power and naval nuclear propulsion, not only in the United States but also in the Soviet Union/Russia and other countries, has created a hesitation to move away from traditional LWR technology. An additional difficulty is the mix of government and industry research into six different design categories under GEN IV. A lack of a clear frontrunner among the six advanced reactor categories has resulted in a diverse set of designs being considered around the

world, with multiple branches of often-unique designs existing within each GEN IV system. Two systems that do have significant research and progress towards commercial operation are the SFR and LFR [3], [4]. The SFR and LFR systems enjoy a significant volume of research and operational history, with around 20 commercial and research SFRs and 15 Soviet and United States Navy submarine LFR and SFR cores having been operated over the past 50 years [5], [6]. It is likely that SFR and LFR research, demonstration and construction will continue to expand over the next few decades as currently planned reactors come online and provide years of operational feedback for design improvements.

A major impact on reactor design for commercial power applications is how best to match power output to its intended electric grid supply and the ability to adjust reactor power in response to electric grid or propulsion demand variation or transients. At the commercial grid level, variable demand for power during stable periods of operation can be managed by supplying base load power from large nuclear plants and variable power by other generating sources. It is also possible to utilize a variety of energy storage technologies (i.e., thermal storage external to the reactor, battery power storage after electricity generation, or diversion of output to other purposes such as hydrogen generation). For naval propulsion, power transients are much more frequent (every few minutes to hours compared to days for commercial plants) and provide a unique motivation for autonomous load following (ALF). Navy nuclear operators experience a much larger demand on active reactor control, leading to more opportunities for errors, misalignments, or inefficient control. ALF would benefit navy reactors with smoother power transient control and less operator induced degradations.

During power transients, reactor power is changed manually or automatically, either using control rods (manually or computer operated) or by inherent reactivity feedback. The process of autonomous load following (ALF) is an idea where a change in output load demand affects the thermal-hydraulics and neutronics of the reactor, which results in changes to the reactivity contributions of the key components of heat and power generation. A change in steam demand involves a change in coolant temperature, affecting the temperature-dependent coolant properties and the rate of change of coolant temperature within the core. A larger rate of change in coolant temperature creates a greater impact on

the total reactivity balance, allowing faster response to load changes. Significant differences regarding autonomous load following can be anticipated between the main liquid metal coolants being considered for liquid-metal cooled fast reactors (sodium, lead, and lead-bismuth eutectic) due to differences in their fundamental physical and neutronic properties.

Therefore, this thesis attempts to answer four questions: (1) what are the physical temperature-dependent properties and neutron interactions of interest for liquid metal coolants in a fast reactor operating in autonomous load following mode? (2) how do these physical and neutronic properties affect coolant-related reactivity feedback? (3) how do different coolants compare in their ALF capability? (4) is there enough of a comparative separation between the coolants considered to impact coolant preference in systems relying on ALF in future reactor designs?

To answer these four questions, a literature review of liquid metal coolant properties and neutron interactions was used to identify the physical properties and neutron interactions most likely to be affected by temperature changes and to have the greatest impact on reactivity addition [7] [8]. Thermal-hydraulic equations developed by Argonne National Laboratory were used to numerically analyze the impact of the selected coolant properties on temperature change within the coolant and their impact on the temperature coefficient of reactivity based on a simplified reactor configuration and typical coolant temperature and mass values [9]. Pb-208 was used for the lead coolant neutron interactions due to its most favorable neutronic properties among the naturally occurring stable lead isotopes; however, the physical properties of lead are not isotope-specific and therefore not expected to differ among the common mix of isotopes in industry grade “pure lead” [10]. The composition of lead-bismuth eutectic is 44.5% lead and 55.5% bismuth [7]. Graphs created from the evaluated nuclear data files (ENDF) provided a qualitative comparison of neutron interaction cross sections for the three most likely interactions with each coolant within the fast neutron spectrum and allowed an extrapolation of neutron hardening and leakage as it impacts ALF [8].

THIS PAGE INTENTIONALLY LEFT BLANK

II. PHYSICS OF FAST REACTOR LOAD FOLLOWING

In order to investigate the reactivity considerations of autonomous load following, a basic understanding of nuclear reactors and neutron interactions with the coolant is required. This chapter covers some basic operations of reactors to include neutron interactions and fission processes, in addition to providing a basic background on fast reactors and the processes involved in load following.

A. REACTOR COMPONENT BASICS

All operating nuclear reactors contain the same basic systems in some configuration, with components and fluid flow being separated into a primary and secondary systems. The primary system containing the fluid that interacts with the fuel both as a coolant and as a medium that either moderates neutron energy (in the case of thermal reactors) or reflects neutrons back to the fuel (in the case of fast reactors). Typical primary components are the reactor core (containing the fuel rods and control rods), primary coolant pumps, heat exchangers, reactor vessel, and one side (the primary side) of the steam generators. The fuel is usually a mix of uranium isotopes, U-235 and U-238. In the case of commercial reactors, most of the fuel is U-238 due to the much greater concentration in nature and limits on enriching the U-235 portion from non-proliferation concerns and cost [1]. Higher levels of U-235 are generally used in military applications to meet the unique requirements and specification of such reactors. Heat is generated from the fission process in the fuel matrices, and this heat is transferred via conduction and radiation to the primary fluid. This fluid is generally also the cooling medium for the reactor, which gives it the common term “primary coolant.” For thermal reactors, water is the most common coolant, and it also serves as the “moderator” to slow down neutrons from their initial high-energy state to a lower, thermal energy state which encourages fission. In fast reactors a moderator is not required and other fluids such as a gas or liquid metals are available for use [1]. As the primary coolant travels through one side of the steam generator, heat is transferred via conduction to the secondary system to a different fluid, usually water, where it becomes steam to turn turbines, for either propulsion or

electric generation. Most commercial and military reactors use water as the fluid in the secondary system. The general components for the secondary side are steam generators, feedwater pumps, heat exchangers, and turbines. As more demand for electric generation is placed on the turbines, more steam is needed from the steam generators, resulting in more heat transfer from the primary to secondary, which causes the primary coolant temperature to decrease and reactor power to increase to provide more fission and heat to balance the system. While the primary and secondary systems have an intricate connection, this thesis will focus on just the primary side without requiring extensive discussion of how the secondary side is operating beyond drawing heat from the primary.

B. NEUTRON INTERACTIONS

The key to successful control and operation of a reactor is maintaining the right balance of neutrons. Neutrons are neutrally charged particles, similar in size and mass to protons. Because of their neutral charge, neutrons do not have to overcome any electrostatic repulsion in order to penetrate a nucleus; they only require enough energy to overcome the strong nuclear force [11]. Neutrons are categorized into three regions based on their energy: “slow” or “thermal” (in this thesis equivalent terms) for kinetic energy below 1 electron Volt (eV), “intermediate” for kinetic energy between 1 eV and 0.01 MeV, and “fast” for kinetic energy above 0.01 MeV [11]. The interaction of a neutron and a nucleus frequently results in either a scattering or absorption event, although other reactions (e.g., (n,2n) or (n, α)) can also occur. Scattering can be elastic or inelastic, while absorption can result in fission or radiative capture. Particle ejection is another possible result of absorption, but fission and radiative capture are the two more important and specifically relevant interactions for this topic.

A key idea that should be explained first is the concept of “cross section.” The method to determine the probability of a neutron interaction occurring is to think of the target nucleus as an effective cross-sectional area in the view of the neutron [11]. This effective cross section is unique for each type of interaction for each target nucleus. The cross sections are so small they have their own unit, barns, with $1 \text{ barn} = 10^{-24} \text{ cm}^2$. Cross sections are very dependent on neutron energy, with this dependence exploited when

choosing different reactor fuels, fluids, and components to either increase or decrease the likelihood of interactions with each material. Another parameter related to cross section is the neutron mean free path. Mean free path is the average distance a neutron travels before interacting with a nucleus and is different for each interaction. This means a neutron may have to travel a shorter distance to experience fission than it does to experience elastic scattering. To summarize, a cross section for scattering or absorption is essentially a physical measure of probability for the interaction occurring when compared to other interactions.

1. Elastic Scattering

Elastic scattering occurs when a neutron either touches the target nucleus and bounces off or gets close to the nucleus and is deflected. The important context for energy consideration is that no energy is transferred into nuclear excitation, resulting in only a change of direction for the neutron and minimal kinetic energy change [11]. This description is a good approximation when the target nucleus is considered to be at rest and is much more massive than the neutron, akin to a marble bouncing off a stationary billiard ball. Elastic scattering is a beneficial interaction for fast reactor coolants because it “reflects” neutrons at high energies back towards the core without losing an appreciable amount of energy from the interaction.

2. Inelastic Scattering

Inelastic scattering is different from elastic scattering because the target nucleus experiences an excitation from the collision, with the neutron either touching the nucleus or entering and exiting at a substantially lower energy [11]. The general result is a reduction in the neutron kinetic energy (reduction in eV), moving from the fast spectrum towards thermal energies. Additionally, the excited target nucleus desires a return to a stable condition and will do this through gamma ray emission. Inelastic scattering is undesirable in fast reactor coolants because it slows down neutrons below the desired fast energy range designed for the fission process.

3. Radiative Capture

Radiative capture is a form of absorption in which a neutron enters the target nucleus and remains there, unlike inelastic scattering when the neutron is then subsequently emitted. This capture of the neutron excites the nucleus into a higher energy state with a mass number increased by one [11]. The new nucleus de-excites through gamma emission, and this results in the heavier isotope returning to its ground state. Except in the case of a breeder reactor (which benefits from the absorption of neutrons to convert fertile nuclei into fissile ones), radiative capture (RC) is undesirable in reactors because it permanently removes a neutron from the total balance available for fission. An additional exception to this is the role of neutron capture in control rods which is important in both thermal and fast reactors.

4. Fission

Fission occurs through the same process as radiative capture, with a neutron being absorbed to form a heavier, excited compound nucleus. Instead of de-exciting through gamma emission, the nucleus may split into two smaller nuclei. In order to fission, the compound nucleus must be excited to a critical energy unique to each isotope [11]. The critical energies of certain isotopes of uranium and plutonium make them favorable for use as fissile materials requiring little to no extra kinetic energy to reach the critical fission energy after absorbing a neutron. A benefit of using fast neutrons for fission is that they bring a higher kinetic energy to enable some isotopes to reach the critical energy for fission that thermal neutrons are unable to provide [11]. An additional benefit is the fact that fissions induced by fast neutrons generally produce more neutrons than fissions induced by thermal neutrons.

C. REACTOR FISSION PROCESS

The fission process takes place as a result of the absorption-fission neutron interaction between a neutron and a fuel particle (U-235 in almost all cases for commercial thermal reactors, other uranium isotopes and different elements as well in planned fast reactors). In the following discussion, U-235 is used to explain how energy is obtained from a fission event in a reactor. Because of the low critical energy for fission in U-235

(5.3 MeV), an absorbed neutron brings the excitation energy level to over 6 MeV and causes fission to occur in 85% of interactions [11]. When the resulting excited U-236 nucleus splits, it forms two fragments of dissimilar size which repel each other with great force and kinetic energy. This energy is a result of the difference in the binding energy per nucleon (the energy required to hold the nucleus together) of the compound nucleus and the fission fragments. The fragments are more tightly bound due to their smaller size, and as a result energy is released to balance the binding energy total of the compound nucleus.

After splitting, the excited fission fragments emit high-energy fast neutrons in the 1–2 MeV range, with an average of 2.5 total neutrons emitted in the first 10^{-14} s from the fission fragments [11]. These are called prompt neutrons due to the immediacy of their birth after fission occurs. The fission fragments remain excited and will decay (emitting gammas and other particulate radiation including protons, electrons and neutrons) to reach a more favorable ground state. These later produced neutrons are termed delayed neutrons and generally have slightly lower kinetic energy depending on the delay time (up to a minute) and fission fragment parent. Delayed neutrons are critical to controllable reactor operation because they sustain the delicate balance of the fission chain reaction over a much longer time frame than prompt neutrons. Consequently, the impact of delayed neutrons is to enable reactor operator control in real time.

The total energy from the fission of a U-235 nucleus is approximately 211 MeV, most of that from the kinetic energy of the fission fragments and the rest from the decay of fission fragments, gamma and neutrino energy, and kinetic energy of fission neutrons [11].

D. THERMAL VS. FAST REACTORS

The basic difference between a reactor labeled as “thermal” and one labeled “fast” is the neutron spectrum required to maintain the fission chain reaction. Thermal reactors rely on slowed down, thermal energy neutrons to maintain the chain reaction of fission, and although a small level of fast fission occurs in thermal reactors, it represents a relatively small contribution to the overall fission balance [1]. Conversely, a fast reactor requires only the fissions from fast energy neutrons to sustain itself and does not require the supplement of energy and neutrons from thermalized neutron interactions to maintain itself in a critical

state. This energy spectrum requirement for each type of reactor results in different characteristics of the fuel and coolant being used together to sustain fission chain reactions.

Figures 1 and 2 show the cross sections for fission and radiative capture for U-235 and U-238, highlighting the opposite fission characteristics of each. U-235 always maintains a higher cross section for fission (N, F) than capture (RC) across all energy ranges, with the only exception the resonance absorption region in the middle of the intermediate energy range where RC and fission exhibit similar probabilities. At the upper energy region, the RC cross section quickly dies off, indicating a much larger relative preference for fission in the fast spectrum as compared to radiative capture, even if the value of the fission cross section is two orders of magnitude lower than at the thermal energy range. U-238 on the other hand shows a two to three order of magnitude lower cross section for fission than RC, until the fast energy spectrum region at 1 MeV. At this point fission is considerably much more likely to occur than RC, reaching fission cross sections similar to U-235. U-238 also has a resonance region in the intermediate energy range but this is of less interest regarding fission prospects in fast reactors because radiative capture was already higher than fission before and after this resonance region and in most fast-neutron systems, neutron energies remain well above the energies of importance for resonance interactions.

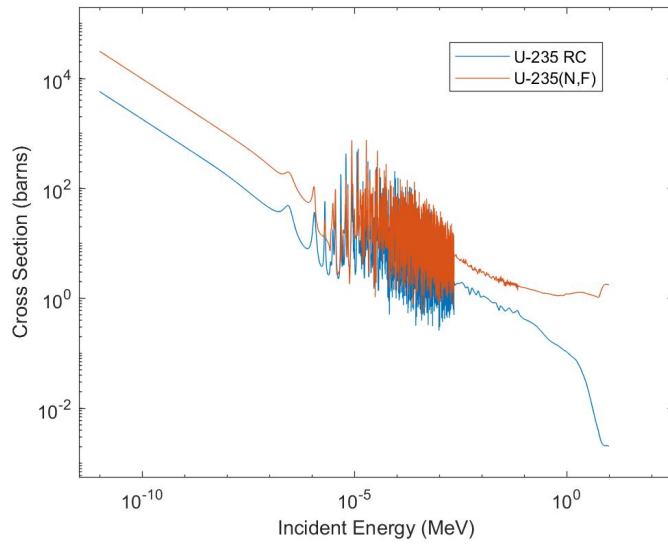


Figure 1. Neutron Cross Sections for U-235. Adapted from [8].

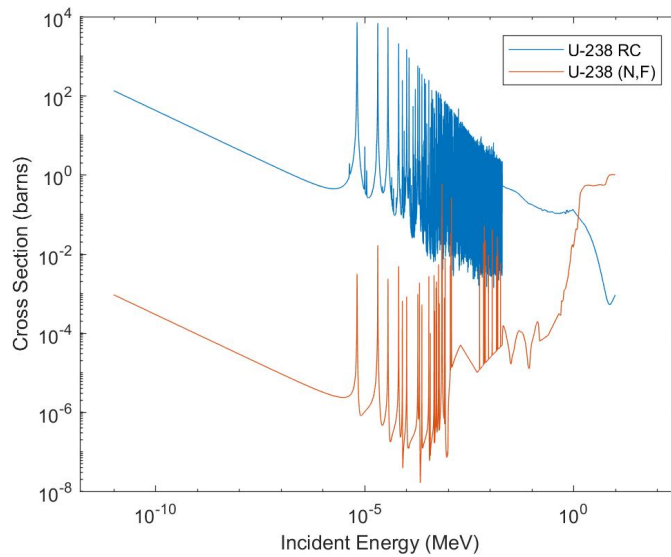


Figure 2. Neutron Cross Sections for U-238. Adapted from [8].

These two figures show the benefit of operating reactors in the fast energy spectrum, where more fuel types become available for fission. In the thermal range, only U-235 is readily available as a naturally occurring fissile material source. U-233 and Pu-239 are also potentially good sources for thermal fission but require man-made production

and therefore significant energy and cost to produce them in sufficient quantity as fuel material [4]. With fast reactors, many more heavy isotopes, including U-238 and actinides, have higher fission cross sections than RC cross sections in the fast energy region. While in some cases the fission cross section values are still lower than those of U-235, making them less likely to interact with a neutron than U-235, their chance of fissioning is still a statistically relevant impact and can contribute to reactor operation. This is of interest to GEN IV reactor designs to reduce the amount of reactor waste produced by one fuel cycle and to use up much of the spent fuel being stored currently as waste [4].

E. CRITICALITY AND REACTIVITY FEEDBACK

The two interconnected terms that summarize reactor operation and safety are criticality and reactivity. Controllable operation of a reactor depends on understanding and predicting the neutron balance in the reactor after each generation life cycle, from when a batch of neutrons are gained to when they are lost. After a neutron is born from fission, there are three “deaths” it can have in relation to the total neutron balance after any scattering interactions: fission, non-fission absorption, and leakage. Fission and non-fission absorption (most commonly radiative capture in the fuel or coolant) have already been discussed, and leakage occurs when a neutron physically leaves the reactor system.

The effective multiplication factor, k_{eff} , is a useful number that relates neutron balance, criticality, and reactivity. Here I will use the letter k to refer to k_{eff} in most equations. This factor combines the probabilities of leakage, scattering, absorption, and fission into one number that is centered around 1.000. If k is equal to 1.000, the fission chain reaction is proceeding at a steady rate where the number of neutrons produced equal the number that are lost each generation and the neutron balance is considered stable [12]. This condition is known as criticality. When k is greater than 1.000, the reactor is supercritical and the neutron balance increases with each cycle of neutrons. For k less than 1.000, the opposite is true with the reactor considered subcritical and the total number of neutrons decreases. Table 1 compares the three conditions of criticality, with their corresponding graphs illustrating the effects of k being less than, equal to, or greater than 1 on the total neutron balance ratio.

Table 1. Criticality Definitions and Graphs. Source [13].

Criticality	Corresponding Explanation	Graphical Representation
Critical	The sum of the neutron absorption and leakage rates is exactly equal to the neutron production rate	<p>A graph showing the number of neutrons on the y-axis (ranging from 0.0 to 2.0) versus the number of neutron generations on the x-axis (ranging from 0 to 16). A horizontal dashed line is drawn at y=1.0, labeled 'k=1'.</p>
Sub-critical	The sum of the neutron absorption and leakage rates is higher than the neutron production rate	<p>A graph showing the number of neutrons on the y-axis (ranging from 0 to 1000) versus the number of neutron generations on the x-axis (ranging from 0 to 16). A curve starts at (0, 1000) and decays exponentially towards zero, labeled 'k<1'.</p>
Supercritical	The sum of the neutron absorption and leakage rates is smaller than the neutron production rate	<p>A graph showing the number of neutrons on the y-axis (ranging from 0 to 300) versus the number of neutron generations on the x-axis (ranging from 0 to 16). A curve starts near (0, 0) and increases exponentially, labeled 'k>1'.</p>

Safe reactor operation keeps the reactor near criticality at all times, with the k value deviating from 1.000 only a few hundredths at a time. This deviation from $k=1.000$ or criticality is referred to as reactivity [12]. Reactivity is defined as the departure from criticality and the fractional change in neutron population per generation [12]. The equation for reactivity is $\rho = (k - 1) / k$. In relating reactivity to criticality, if reactivity equals zero, then $k=1.000$ and the reactor is critical. A reactivity less than zero relates to subcriticality and a reactivity value greater than zero relates to supercriticality.

Adding to the complexity of defining reactivity, several different units are utilized by different communities of scientists, industry, and military. There are four most common units used to represent reactivity. From the equation $\rho = (k - 1) / k$, the units $\Delta k / k$ result and are called units of reactivity [12]. Sometimes the terminology $\Delta\delta / \delta$ is also seen in older texts or U.S. Navy applications, but for present purposes, we will utilize $\Delta k / k$ for continuity here. The units $\Delta k / k$ are considered the most basic units, and generally all other

units relate to them. Related units are pcm, where $1 \text{ pcm} = 0.00001 \Delta k / k$ (common in nuclear engineering research) and $10^{-4} \Delta k / k = 0.0001 \Delta k / k$. The $10^{-4} \Delta k / k$ units are used by navy nuclear propulsion operators to allow reactivity to be expressed in whole numbers and to allow for easier representation and simple math. The fourth version of reactivity units are dollars and cents [12]. One dollar is equivalent to the delayed neutron fraction and equates to the reactor being in a prompt critical condition, which means that criticality is maintained solely by prompt neutrons and can result in rapid and uncontrollable power excursions. A cent is one-hundredth of a dollar. Reactivity equaling zero dollars is a criticality condition ($k=1.000$) with the cents representing the delayed supercriticality of the reactor until reaching prompt critical at one dollar [12]. These units are more commonly used in commercial and research reactors. There is no direct conversion between dollars and cents and the other units of reactivity, and therefore reactivity units will be represented here in the format from the source from which they were obtained.

The final concept related to criticality and reactivity to understand is reactivity coefficients. Each component in a reactor contributes to the total reactivity, with each component's contribution summed to result in a final, total reactivity that defines criticality. Reactivity coefficients are the amount of change in reactivity given a change in a parameter [12]. This relates the changes in the physical properties of components such as the coolant and fuel to the reactivity balance of the reactor. The reactivity coefficient unit is typically α_x , with x being the parameter that is changing. Reactivity coefficient is related to the change in reactivity by the equation $\alpha_x = \Delta\rho / \Delta x$. The more useful form during reactivity calculations is called the reactivity defect and is characterized by the equation $\Delta\rho = \alpha_x \Delta x$ [12]. If $\Delta\rho$ increases for an increase in parameter x, then the reactivity coefficient is positive; if $\Delta\rho$ decreases for increasing x, then the reactivity coefficient is negative. Figure 3 shows the impact of positive and negative reactivity coefficients on total reactivity and reactor power. Large coefficients, either positive or negative, can quickly drive a reactor into an uncontrollable supercritical condition or shutdown if not balanced appropriately by other factors.

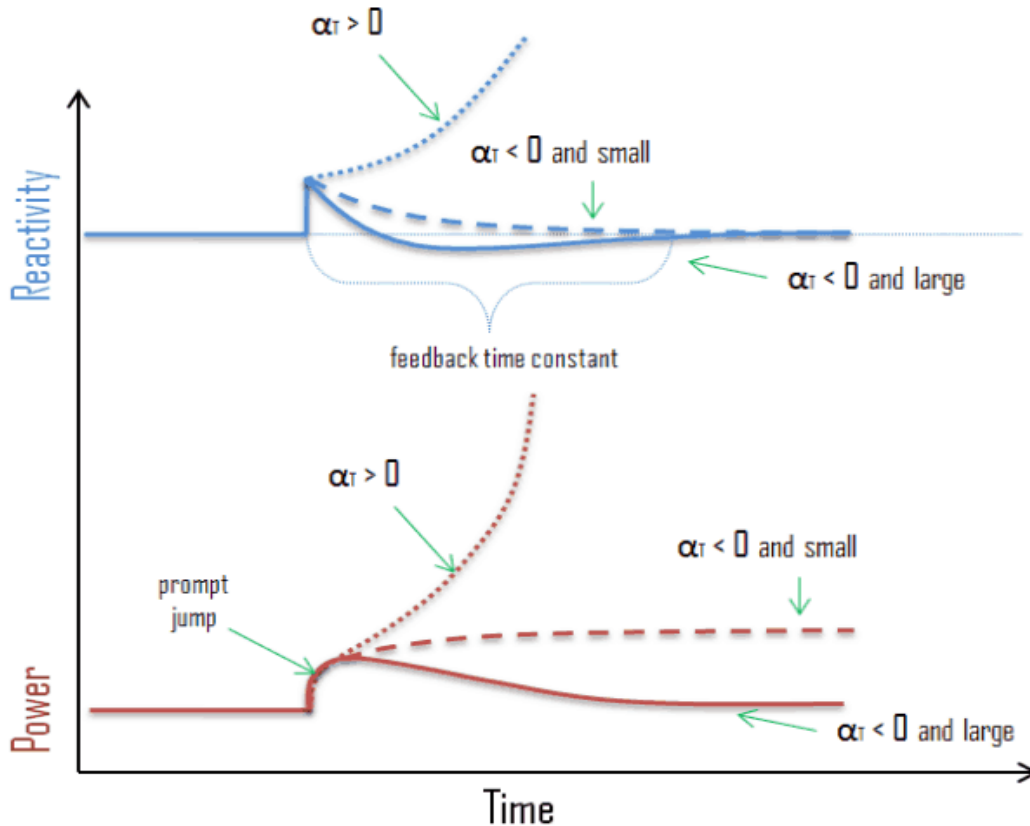


Figure 3. Reactor Power and Reactivity vs. Time for Different Reactivity Coefficients. Adapted from [12].

There are several reactivity coefficients that dominate the reactivity balance of the reactor, some of them being coolant temperature, fuel temperature (also called Doppler broadening), component expansion, pressure, void, poisons, and control rods [12]. Not all are present in every reactor based on the coolant and fuel types and whether it operates in the thermal or fast region. Additionally, while some coefficients are always positive or negative, reactor design dictates whether others (such as coolant temperature) are positive or negative for that reactor. The reactivity coefficients of interest in this thesis are the coolant temperature (sometimes characterized as thermal expansion of the coolant) and Doppler broadening. Some research shows that the Doppler broadening coefficient can have a 4–5 times larger impact than coolant temperature on reactivity in oxide-based fuels but nearly equal impact in metal fuels [14]. While all data in this thesis will consider reactors and simulations using only oxide fuels, it will be important to remember the greater

impact that coolant reactivity consideration will have in metal fuel reactors in coolant design selection.

F. REACTOR CONTROL AND LOAD FOLLOWING

The three questions to answer regarding autonomous load following are: (1) what is ALF? (2) why should ALF be a topic of interest in future reactors? and (3) what factors influence ALF the most?

Reactor control exists in two basic forms for operation, manual and autonomous. Reactor shutdown often involves a different method or additional supplements to control rods for slow or emergency shutdowns and will not be discussed because of the absence of load following to that operation. Manual operation is through the use of control rods, either in response to a power demand change or a planned power change, usually to maintain the temperature of the coolant within a specified band. U.S. Navy reactors are operated in manual operation to respond to changes in propulsion speed or in preparation for aircraft launches. Control rods for normal operation and power transient response change height to expose more or less fuel to change the amount of total fissions in the core and change the reactivity balance and coolant temperature until steady state is reached again. Autonomous control means that the reactor power follows the steam demand from the power conversion turbines. This control can be through the use of pre-programmed or computer-controlled control rods or through passive reactivity response. Some literature considers non-operator-initiated control rod movement to be autonomous load following (ALF) but that definition does not encompass the same idea as passive reactivity response and so is discarded for this thesis. To clearly state, the term autonomous load following here means that the reactor responds to a change in steam demand and reactor power through reactivity defects based on the changing conditions within the core to achieve a new critical steady state condition.

The European Utility Requirements (EUR) has set some requirements for modern reactors regarding load following. The primary requirements are that they can continuously regulate their power between 50% and 100% of total rated power, up to the 90% point in their fuel cycle [15]. One benefit of the focus of the GEN IV forum on mostly fast reactor

designs is that they eliminate several problems with ALF that light water thermal reactors (LWR) face [1]. LWR are “susceptible to Xenon poisoning, axial power oscillations, and are sensitive to burnup” [15]. These three problems are almost completely eliminated from fast reactors for the majority of core life due to changes in cross sections in the fast spectrum, better temperature feedback regulation, and long fuel life expectancy [15].

There are many reasons that ALF is a topic of interest in future reactor designs. One reason is because many countries have significantly increased the share of nuclear power in their national electricity mix and require the ability to adapt the electricity supply to power demand throughout the day [16]. A second point is that many reactors in operation today are older designs that were not designed with autonomous load following in mind. While most of these reactors can produce some limited form of load following action, they are not as efficient as newer designs that are centered around ALF operation [16]. Finally, even in countries where nuclear power is not the largest share of power production, with the increase of intermittent sources such as wind and solar on grids that are shared with nuclear power plants, the reactors must be able to react to the constant changes in power production from these intermittent sources [16].

A relatively recent method of passive reactivity control is the ARC system. This system is primarily designed to ensure safety during accident scenarios but has also been considered for long term reactivity changes in a load following reactor [15]. It works by connecting a reservoir of a neutron poison to the coolant that responds to temperature changes within the core. It was proven through simulation that this method of control was effective for load following water and metal cooled reactors and could be of use in future GEN IV designs in coordination with the selection of the best load following coolant [15].

Many factors can affect the capability for a reactor to perform load following. Some of the negative factors with LWR were already discussed, such as Xenon poisoning and fuel burnup. Additional factors relate to the operating and safety margins designed into the reactor. The larger the allowable temperature difference between the inlet and outlet coolant temperatures, the more room for passive reactivity response to occur before a temperature limit is reached. While LWR typically have a ΔT between the hot and cold legs of only 10–20 K, liquid metal coolant fast reactors are designed with a ΔT in the 100–

175 K range. This significant increase in temperature operating band allows time for normal transients in the 5–10% power change range occur and come back to new steady state conditions. The general consideration of how anything affects ALF is how a change in material property affects the rate of reactivity change. The co-dependent properties of coolant temperature and density, heat capacity, thermal conductivity, and viscosity will be the focus of this research.

III. PROPERTIES OF COOLANTS

There is no dominant physical or neutronic property of the considered coolants that could result in an easy selection as a preferred reactor coolant to meet the requirements of the GEN IV forum. While there are many other liquid metals that could theoretically be possible for consideration as reactor coolants (such as gallium, tin, potassium and lithium), experience with historical reactors, prototypes and design analyses lead to a consensus that lead, sodium, and LBE are the prime liquid metal options going forward [1]. In this chapter the physical and neutron interaction properties of these primary coolants are described.

A. PHYSICAL PROPERTIES

The heat transfer properties of liquid metals make them superior to water as reactor coolants for fast reactors, in addition to the reduction in the moderating effect on neutrons to thermal energies which is undesirable in fast reactors. Table 2 summarizes the basic properties of each coolant at a representative operating temperature (i.e., 723 K). The impact of temperature-dependent variations of the properties of these coolants will be explored throughout this chapter. Note that the graphs for LBE are often unsurprisingly similar to those of lead, with a slight vertical shift in the parameter values being a result of the bismuth portion of the mix.

Table 2. Thermophysical Properties of Liquid Metals.
Adapted from [7].

Properties	Na	Pb	Bi	LBE
Atomic Number	11	82	83	--
Atomic Mass	22.99	207.2	208.98	--
Melting Point (K)	371	600.6	544.6	398
Boiling Point (K)	1155	2021	1831	1927
Density (g/cc)	.8441	10.52	--	10.13
Thermal Conductivity (W/(m*K))	70.02	17.15	--	13.77
Heat Capacity (J/(kg*K))	1272	145.8	--	142
Viscosity (Pa*s)	.00025	.002	--	.0013

1. Melting and Boiling Points

A relatively low melting point is generally a desirable characteristic since it reduces the likelihood of unintended freezing while increasing the safety margin between the minimum coolant operating temperature and the melting point of the coolant. Should the coolant temperature decline to reach the melting point, this would enable the formation of solid coolant material and the possibility of clogging channel tubes and creating localized hot spots exists due to a reduction of localized heat removal. These hot spots could lead to fuel and cladding failure as the heat from fission is unable to dissipate, causing fuel melting and containment failure at these points. This would result in the release of fission products and fuel material into the coolant, which will raise the overall radiation level in the primary loop, cause a higher risk to operators, and increase the chance of radionuclides being released into the environment from primary coolant leakage or discharge. Additionally, a higher melting point may require an auxiliary heating system to be incorporated to maintain the coolant in a liquid state prior to startup and during extended shutdown. This increases the operational and equipment complexity associated with reactor startup and other activities related to plant shutdown conditions.

Sodium and LBE are strong candidates as liquid metal coolants due to their relatively low melting points. While not quite at ambient temperature, they are within the temperature range that can be readily maintained in the short term by post-shutdown decay heat generation. This allows the coolant to remain liquid and thus facilitates quick restart following a minimal length shutdown, such as a vessel might experience during a port visit or planned maintenance work. Due to the significantly higher melting temperature of pure lead, lead-cooled reactors would require dedicated heating systems for startup or low temperature operations. One benefit of lead's higher melting point is that, in the event of a reactor vessel or other leak, the released coolant will quickly cool and harden, providing localized containment and possibly sealing the leak.

On the other extreme, a high boiling point is also desired to reduce the uncontrollable reactivity increase and reduced heat transfer effectiveness of boiling liquid metals. For these considerations, lead and LBE are highly favored because their boiling points far exceed the operating parameters of fast reactors and provide significant safety

margins in the event of a casualty and resulting temperature spike. Sodium's boiling point is low enough that for some accident or transient conditions, portions of the coolant could reach boiling conditions that could result in a significant additional degradation of safety.

2. Density

Density (ρ) is a measure of the ratio of a materials mass to the volume it displaces. Density reduction with increasing temperature means fewer molecules and nuclei in the same volume of space as compared to its condition at lower temperature. This affects the mean free path of neutrons by increasing the distance travelled by neutrons before having a scattering or capture event with a coolant nucleus [11]. This neutron transport distance increase can increase the chance for the neutron to "leak" out at the boundaries, escaping the coolant and fuel by reaching the other reactor vessel components or atmosphere and being absorbed there. Within the core, the increased mean free path tends to result in more fast fissions because neutrons have a higher chance to reach a fuel nucleus and fission before encountering a radiative capture event with the coolant or cladding or slowing down to thermal energies from scattering events [14]. Table 2 showed the average density of sodium to be approximately a factor of 10 less than that of lead or LBE, with Figure 4 showing that the density for all three coolants falls linearly with increasing temperature but maintains a roughly 8 to 10 times difference between sodium and lead/LBE over the normal operating temperature range of a fast reactor.

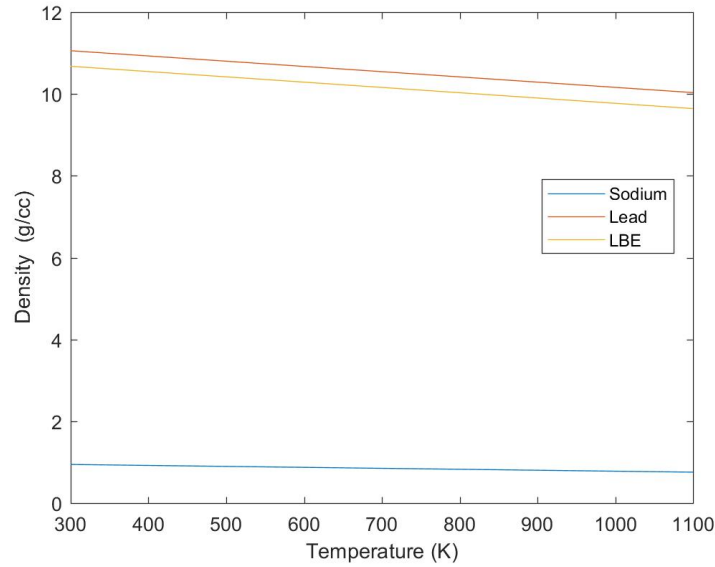


Figure 4. Temperature Effects on Density of Coolants.
Adapted from [7].

The empirical equations for density in the operating temperature range with results in units of kg / m^3 are as follows [7]:

$$\text{Sodium} \quad \rho(T) = 1014 - .235T \quad (1)$$

$$\text{Lead} \quad \rho(T) = 11441 - 1.2795T \quad (2)$$

$$\text{LBE} \quad \rho(T) = 11065 - 1.293T \quad (3)$$

Sodium has a slightly more consistent density profile through the temperature range, with lead and LBE decreasing somewhat more rapidly. However, lead and LBE maintain a significantly higher density throughout the operating range by approximately an order of magnitude compared to Sodium.

3. Thermal Conductivity

Thermal conductivity (λ_c) is the measure of a material's ability to conduct heat, with heat transfer occurring slower in low thermal conductivity materials than ones with a high thermal conductivity property. The units used are $W / (m * K)$. Water has a very low value (0.6) compared to liquid metals, which contributes to the preference for liquid metals

in fast reactors, in addition to consideration of the moderating properties of water [7]. This is important because the function of a reactor is to use the heat generated by the fission process to heat water in steam generators, so a higher thermal conductivity in the coolant results in a higher efficiency of moving the heat from the fuel to the steam generators. Figure 5 shows the thermal conductivity of the selected liquid metal coolants. It is easy to see that each of the coolants has at least an order of magnitude higher thermal conductivity compared to water's value of 0.6, with sodium starting at a significantly higher value at lower temperatures.

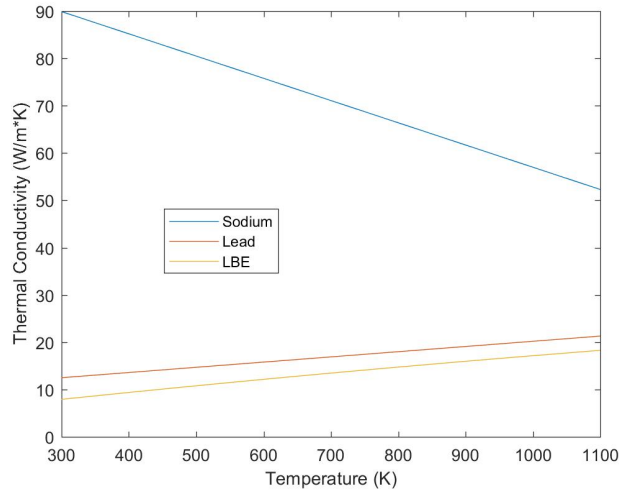


Figure 5. Temperature Effects on Thermal Conductivity of Coolants. Adapted from [7].

The empirical equations for thermal conductivity in the operating temperature range are as follows [7]:

$$\text{Sodium} \quad \lambda_c = 104 - .047T \quad (4)$$

$$\text{Lead} \quad \lambda_c = 9.2 + .011T \quad (5)$$

$$\text{LBE} \quad \lambda_c = 3.284 + .01617T - (2.305 * 10^{-6})T^2 \quad (6)$$

Lead and LBE follow increasing linear lines as temperature goes up, making them better heat transfer mediums at higher temperatures than lower. This is why some advanced reactor designs focusing on lead and LBE coolants have proposed operating temperatures much higher than common designs [1]. Conversely, sodium thermal conductivity drops significantly over the considered temperature ranges. Even with a steep negative slope, however, sodium still maintains a 40–50 unit advantage over lead and LBE through the 700–900 K temperature range most coolants operate at during normal operation.

4. Specific Heat Capacity

Heat capacity (c_p) is the ratio of heat added or removed from a material to the temperature change that results, with specific heat capacity simply being the heat capacity per unit mass of the material. The units for specific heat capacity are $J/(kg * K)$. Heat capacity is based on the degrees of freedom available within the material for thermal energy storage. Since it is assumed that the coolants will all be in liquid form and far enough from freezing or boiling to ignore any quasi-state effects, each coolant has the same number of degrees of freedom. For many thermodynamic based calculations, enthalpy is the measure of energy used. Enthalpy is strongly influenced by heat capacity, so having a good representation of heat capacity is important in determining the energy transfer within the coolant. Figure 6 shows the specific heat capacity profiles of the liquid metal coolants within the sodium liquid temperature range.

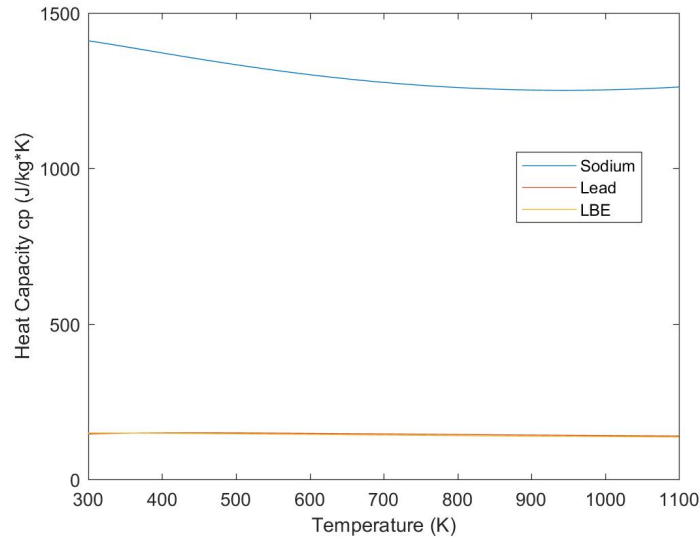


Figure 6. Temperature Effects on Specific Heat Capacity of Coolants. Adapted from [7].

The empirical equations for specific heat capacity are as follows [7]:

$$\text{Sodium} \quad c_p = (-3.001 * 10^6)T^{-2} + 1658 - .8479T + (4.454 * 10^{-4})T^2 \quad (7)$$

$$\text{Lead} \quad c_p = 176.2 - (4.923 * 10^{-2})T + (1.544 * 10^{-5})T^2 - (1.524 * 10^6)T^{-2} \quad (8)$$

$$\text{LBE} \quad c_p = 164.8 - (3.94 * 10^{-2})T + (1.25 * 10^{-5})T^2 - (4.56 * 10^5)T^{-2} \quad (9)$$

The lead and LBE equations have nearly identical profiles because the lead in the LBE dominates the heat capacity characteristics compared to the bismuth portion. It is interesting to note that while the sodium equation exhibits a negative slope and approaches a minimum value around 850 K, the lead and LBE have constant specific heat values regardless of temperature change (in this range). Unlike the case of thermal conductivity, sodium has a significant disadvantage in terms of energy storage compared to lead and LBE at all points in its liquid phase. Sodium requires significantly more energy input to change temperature, meaning that a change in coolant temperature occurs more slowly for sodium compared to lead or LBE. While this is advantageous for transporting heat from the fuel region to the steam generators with the lowest drop in temperature, it is less

desirable with respect to quickly changing coolant temperature in response to power changes in the core.

5. Viscosity

Viscosity (η) is the resistance to flow between adjacent fluid layers, commonly thought of as the thickness of a fluid. The units of viscosity are $Pa*s$. In a reactor, viscosity affects the mass flow rate of the coolant in tube channels or circulation in a coolant pool. A more viscous fluid requires more pumping power to achieve the same flow rate as a less viscous medium, leading to increased demands on the reactor support components. As Figure 7 shows, however, the higher viscosity of lead and LBE lends itself well to concepts of pump-less natural circulation fast reactors that instead use gravity and heat convection properties to encourage constant flow [4].

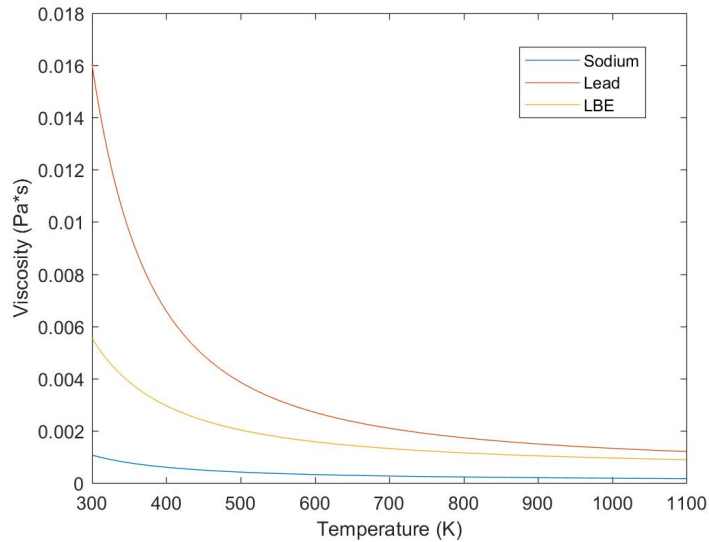


Figure 7. Temperature Effects on Viscosity of Coolants. Adapted from [7].

The temperature dependent empirical equations for viscosity are as follows [7]:

$$\text{Sodium} \quad \eta(T) = e^{(556.835/T - 3958 \ln T - 6.4406)} \quad (10)$$

$$\text{Lead} \quad \eta(T) = (4.55 * 10^{-4}) e^{(1069/T)} \quad (11)$$

$$\text{LBE} \quad \eta(T) = (4.94 * 10^{-4})e^{(754.1/T)} \quad (12)$$

The three coolants all approach a minimum asymptote at higher temperatures, supporting the general understanding that hotter liquids flow faster than slower ones. From Figure 7 it can be seen that at all temperatures lead has the highest viscosity, with LBE and then sodium having a lower resistance to flow. The viscosity effects on mass flow rate requirements and the rate of heat transfer are considered in the next chapter as part of the coolant temperature equation analysis.

6. Physical Properties Summary

For each physical property discussed, there is clear separation between sodium and lead/LBE. Figure 8 indicates the desired region for each physical property as it relates to liquid metal coolants in fast reactors.

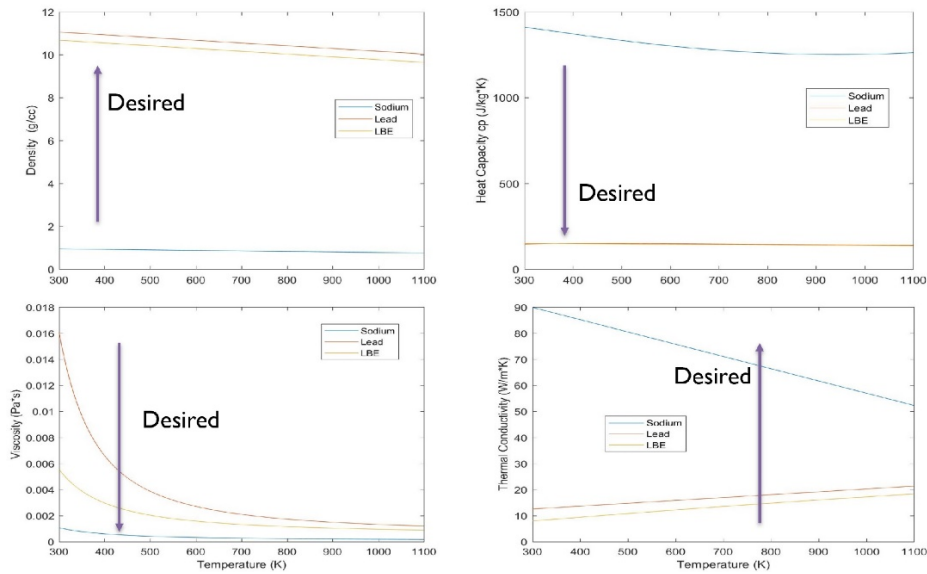


Figure 8. Desired Regions for Liquid Metal Coolant Physical Properties

Figure 8 highlights the split between the coolants, with sodium having more desirable characteristics in regard to viscosity and thermal conductivity but lead and LBE owning the advantage with respect to density and heat capacity.

B. LIQUID METAL COOLANT NEUTRON INTERACTION PROPERTIES

Drawing from the introduction of neutron interactions in the previous chapter, this section looks at the different relevant neutron interactions (radiative capture, elastic scattering, and inelastic scattering) for liquid metal coolants, discusses their impact on reactor dynamics, and compares each coolant based on the most probable neutron interactions. The absorption-fission interaction is not considered because none of the metal coolants are considered fissile sources and each have an essentially impossible chance of neutron-induced fission around the 1 MeV energy range. Bismuth 209 is used in place of LBE in these graphs because they are adapted from data obtained from the Evaluated Nuclear Data Files (ENDF) [8] and are limited to only having single element isotopes available. Although the eutectic mixture of lead and bismuth (LBE) consists of a single mix of lead and bismuth by weight (i.e., 55% Bi and 45% Pb), no ENDF data file has yet been created to specify the neutron interactions of LBE. Additionally, there is no data file for inelastic scattering interactions for Bi-209 and neutrons, and, as a result, only lead and sodium are presented in the inelastic scattering graph shown later in this chapter. While the ENDF has data for energies as low as 10 peV, only values for the fast energy range are presented to provide clearer definition of the cross sections at the fast energies relevant to this research. The main question to be considered with each coolant and neutron interaction is how it affects a fast neutron returning to the fuel to cause fission. Autonomous load following is more effective when the neutron balance remains high as it is affected by changes in physical properties.

1. Neutron Interaction Summary by Coolant

It is interesting to note in Figures 9 and 10 that below a certain energy for each isotope the radiative capture and inelastic scattering cross section lines merge and essentially have the same probability of occurring. Due to lead's nearly equal weighting in LBE and Bi-209 having similar cross section profiles to Pb-208, it can be inferred that there is likely a similar energy for Bi-209 and LBE below which the cross sections for radiative capture and inelastic scattering are the same. The distinction between them below that energy is relatively unimportant for this topic because if the neutron experiences either

interaction it is essentially lost from the fission process due to either being captured or slowing down below the fast spectrum.

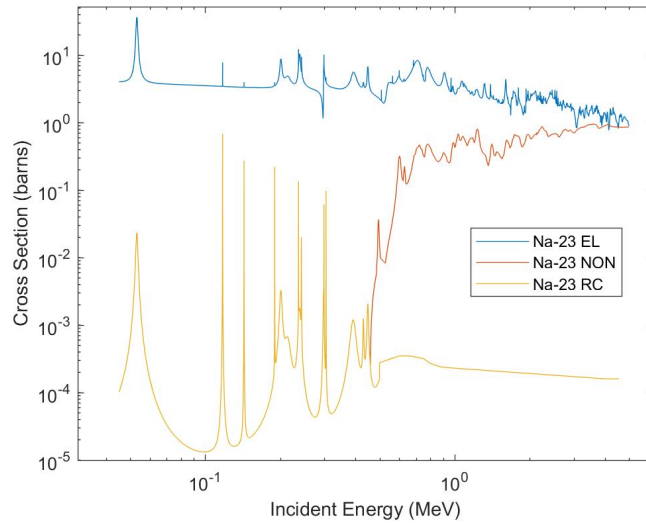


Figure 9. Neutron Interaction Cross Sections for Sodium – 23.
Adapted from [8].

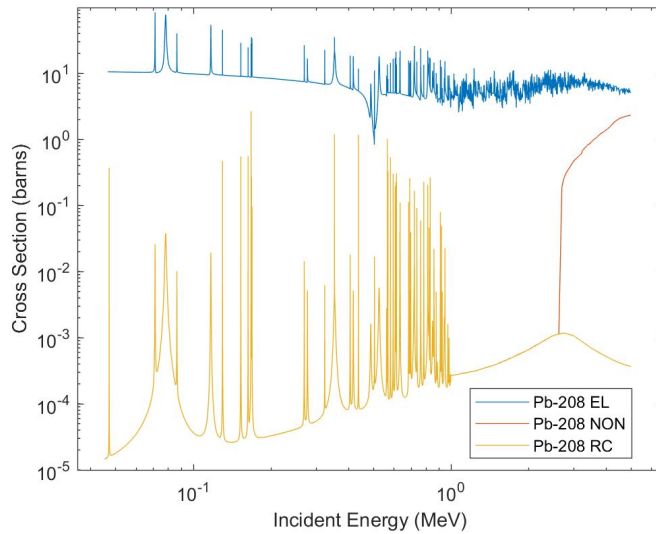


Figure 10. Neutron Interaction Cross Sections for Lead – 208.
Adapted from [8].

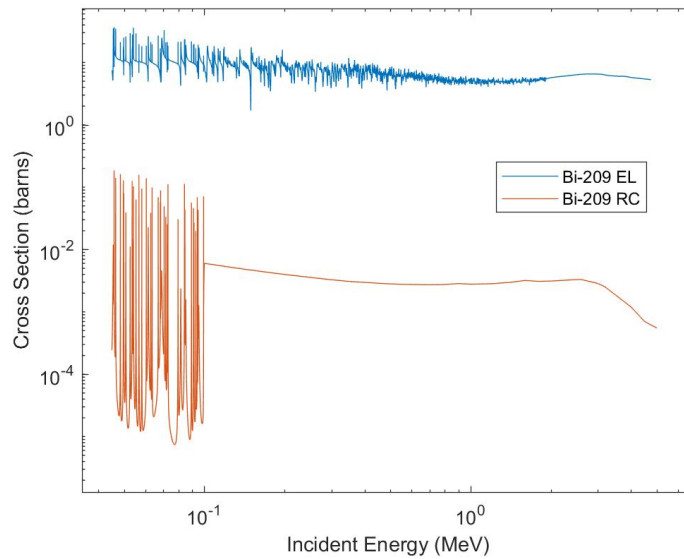


Figure 11. Neutron Interaction Cross Sections for Bismuth – 209.
Adapted from [8].

Figures 9, 10, and 11 each show an important aspect of liquid metal coolants: namely, that elastic scattering (and the potential for neutron reflection back into the fuel zone) is the most likely interaction to occur at fast energies (.05 MeV to 10 MeV). This strong reflection characteristic with relatively little energy loss for the neutron is an important consideration in enabling the fission process to sustain itself through each neutron life cycle. Even when the cross section for inelastic scattering approaches that of elastic scattering at higher energies, as it does in Figure 9 for sodium, there is still a large separation between the scattering interactions and loss due to radiative capture. Additionally, for sodium, the higher inelastic scattering probability occurs at high enough energies that a neutron could remain in the fast spectrum and fission after an inelastic collision.

2. Radiative Capture Comparison

In terms of the fast fission process, any neutron interaction that results in radiative capture (RC) is a loss and undesirable. Figure 12 highlights the separation between the three coolants in the fast energy spectrum above 1 MeV, with bismuth having a higher RC cross section than lead or sodium. Even with the variability in the cross sections below 1

MeV, bismuth still consistently reflects the highest cross section with the exception of variable narrow resonance peaks.

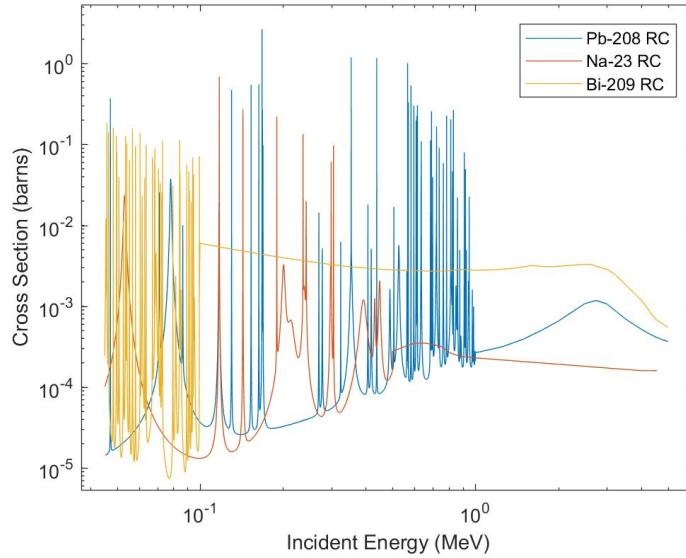


Figure 12. Radiative Capture Cross Sections of Coolants. Adapted from [8].

This multi-magnitude separation between sodium and lead with bismuth clearly makes LBE the least preferred coolant in terms of RC properties, especially at the lower ranges of the fast spectrum (0.1 MeV to 1 MeV) where the capture cross sections for bismuth are constant, and those of sodium and lead vary widely across energies.

3. Elastic Scattering Comparison

Elastic scattering is the most desired interaction for a fast fission coolant in order to return neutrons to the fuel at the highest energies possible, which leads these fast fission coolants to be considered good reflectors. Figure 13 shows how similar each coolant is with respect to elastic scattering cross sections, with minimal separation between lead and bismuth for the entire spectrum. Sodium has a lower cross section than lead or bismuth but is still within a half magnitude at all fast energies until diverging at the higher energy limit.

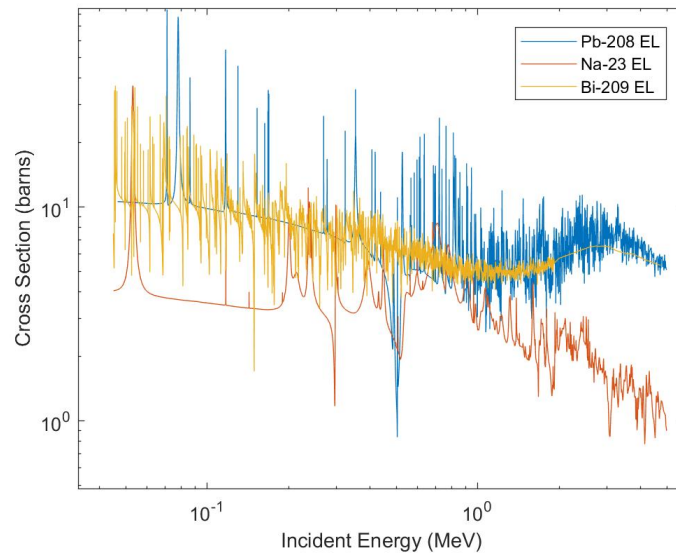


Figure 13. Elastic Scattering Cross Sections of Coolants. Adapted from [8].

Overall each liquid metal makes an excellent reflector based on elastic scattering properties and there is not enough separation between the three in the fast spectrum to choose one as the better choice on this property alone.

4. Inelastic Scattering Comparison

Inelastic scattering results in slower neutrons, leading to a reduced chance of fast fission and more likelihood of leakage or resonance capture at lower energies [11]. Figure 14 illustrates two regions of comparison for lead and sodium, with both metals exhibiting approximately the same cross sections until the 1 MeV point. After 1 MeV, the inelastic scattering cross section of lead remains in the 10^{-3} barns region while that of sodium jumps to just below 1 barn, until at 4 MeV, the cross section for lead jumps to match that of sodium. The inelastic scattering cross section of LBE can be inferred from previous relationships to exhibit similar properties to lead and would likely retain a low cross section until 4–5 MeV as well.

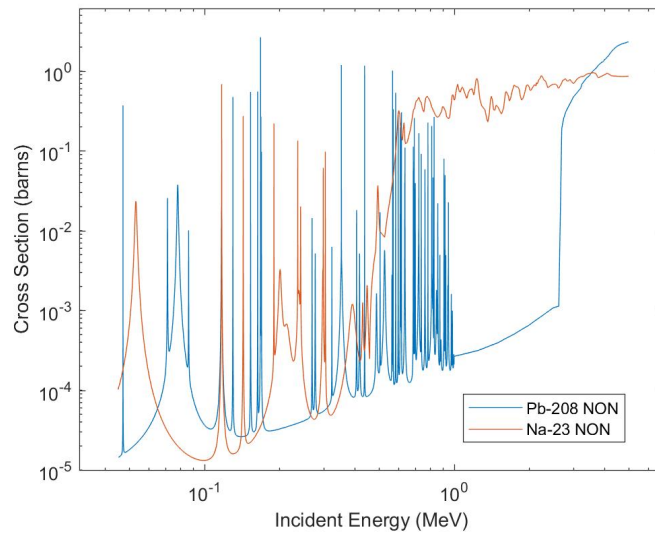


Figure 14. Inelastic Scattering Cross Sections for Coolants.
Adapted from [8].

Since neutrons are mostly born near or above 1 MeV, the multi-magnitude separation above 1 MeV between sodium and lead/LBE makes lead and LBE preferred in regard to maintaining fast neutron population [11]. While LBE properties are being inferred from the lead portion and other neutron interactions of bismuth, this is just one of many consideration points for choosing a fast spectrum coolant.

THIS PAGE INTENTIONALLY LEFT BLANK

IV. PROCEDURE AND RESULTS

In order to achieve the objectives of this thesis, a graphical analysis based on established modeling equations was deemed the best way to analyze and represent the effects of a large temperature range on different parameters and allow easy comparison between reactor coolant types. To create the graphs used, design data relating to coolant type, inlet/outlet temperatures, flow rate, and core dimensions were obtained from multiple publication sources, both scientific and industrial. Once a sampling of data was obtained, a methodology was identified that could enable analysis of different reactor designs and produce graphical representations of the results. Since the focus was limited to coolant and temperature effects, complex codes and models were not needed. Additionally, most of the codes available required more detailed and proprietary reactor design information than is available for most reactor concepts under current development, and the available data were often relevant only to a specific reactor design.

As a result, this research relied on a report by Argonne National Laboratory that provides most of the generic reactor heat transfer equations that could be adjusted for different coolant types and core dimensions and easily graphed using MATLAB [9]. This section summarizes the information gathered, explains the main equations utilized, and presents the results graphically. The following section will provide analysis of the graphs in conjunction with the physical and neutronic properties presented in the previous sections.

A. DATA GATHERING

The process of answering the questions to be addressed in this thesis was challenging due to the diversity and sometimes inconsistency of information available regarding fast reactors. One problem encountered is the difference in reactivity units used by different reports and manuals, preventing direct comparison or ready conversion to comparable units. Another difficulty lies in obtaining enough information about specific reactor designs to use in modeling equations, especially when the designs are proprietary and only limited specifications are released in publicly available reports. Finally, because

many of the previously operated fast reactors were military related, the data available for them beyond some generic fuel and coolant type and power output is highly limited.

Once the physical and neutronic properties of the coolants were collected, the main focus for gathering the remaining data was to find reactivity coefficients of temperature or related reactivity additions from temperature change for power transients. Additionally, it was necessary to find this data for a mix of reactors that were either sodium-, lead-, or LBE-cooled to provide useful comparison. Finally, the heat transfer equations require flow rates, cladding and rod diameters, numbers of fuel rods, and other core dimensional parameters. Data was sourced only for reasonably comparable reactor designs in order to conduct valid analyses (i.e., vertically oriented fuel rods with either pumped or natural circulation coolant flow). Table 3 highlights the reactivity related data found for some different reactor designs.

Table 3. Temperature Dependent Coolant Reactivities

Reactor	Coolant Type	Reactivity	Notes
SPARC [16]	Sodium	-0.89 (BOL) to -0.29 (EOL) pcm/K	Over range of core life cycle.
LFR simulator [17]	Lead	-1.23 pcm/K	
SSTAR [18]	Lead	+ 14¢	Max positive reactivity added from power transient 100% to 0% to 100%. Negative reactivity coefficient.
STAR-LM [19]	Lead	+ 27¢	Max positive reactivity added from power transient 100% to 0% to 100%. Negative reactivity coefficient.
MIT/INEEL simulator [20]	LBE	+0.04 ¢/K	Value at 725°C, Decreases towards zero at lower temperatures.
IFR [20]	Sodium	+0.18¢/K	Unspecified integral fast reactor design
ARC-100 [21]	Sodium	-0.23 ¢/K	

The positive reactivity addition for the two lead-cooled reactors, SSTAR and STAR-LM, from a down-power transient indicate that they have negative temperature coefficients of reactivity. This is consistent with most modern reactor designs requiring negative temperature coefficients to reverse increasing power spikes from transient conditions. The IFR design was the only one with a significantly positive temperature coefficient of reactivity, though little design detail was provided beyond the mention of this reactivity value in comparison to the LBE simulator in the same paper [20]. Figure 15 provides an example of how much temperature (through its relationship with density) can impact the reactivity contribution from the coolant. The three lines in Figure 15 represent the core at beginning-of-life (BOL), mid-life (B=50MWd/kg), and end-of-life (B=75MWd/kg) conditions.

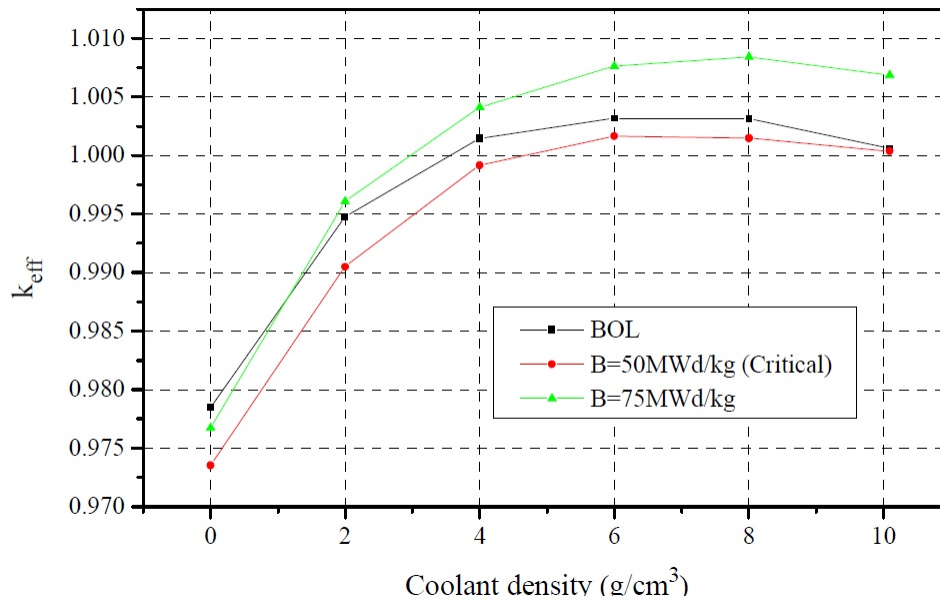


Figure 15. Change in Reactivity for LBE-Cooled Reactor Based on Density Change. Source [20].

Some common-sense interpretation is required as well to recognize that while Figure 15 shows k_{eff} reaching down towards .975-.98 as density approaches zero, the density of LBE will never reach below 9.5 g/cc. This is because it would require the temperature of the coolant to be over 1700 K to have density below 9.5 g/cc, which is well

above any reactor operating range and will have already resulted in significant cladding and fuel damage prior to reaching this point.

In addition to reactivity related data, core dimension elements for sodium-, lead-, and LBE-cooled reactors were each obtained to input into the MATLAB code. The design information was obtained from design plans for three different fast reactors: ARC-100 (sodium), STAR-LM (lead), and SVBR-75 (LBE) [9], [21], and [22]. ARC-100 is a sodium-cooled design based on advances and operational experience from the EBR-II design, with the goal of being an factory-produced reactor with fixed costs that could be easily shipped around the world to any location [9]. STAR-LM is lead-cooled small modular reactor concept developed by Argonne National Lab that could be transported to developing nations with growing electric grids and transient load conditions [21]. The Russian SVBR-75 LBE-cooled design focuses on passively safe behavior, accident impact reduction, and lowered capital costs and construction time [22]. Each reactor type was designed to optimize the coolant selected. By replacing the coolant data with the other two coolant types for each reactor, it is possible to show the effects on the change in heat transfer rate from choosing different coolant types. This ensured that the resulting graphs would have a representative selection of comparison data by including a reactor designed specifically for each coolant.

B. MODELING EQUATIONS

The overall concept of load following in fast reactors has been proven in practice and theory, which meant that a larger system code was not needed to re-prove the process again [16]. Additionally, many of the larger full-scale thermal-hydraulic and neutronic codes require significant modification and input data to model specific reactor designs. To do a smaller scale analysis and comparison of just the three coolant types considered, their ability to affect the coolant temperature change rate (and therefore the response time of coolant temperature induced reactivity addition) was chosen as the most direct comparison tool. Figures 16 and 17 show the general reactor design model for coolant flow through the core and the separation of the core region into time dependent temperatures nodes.

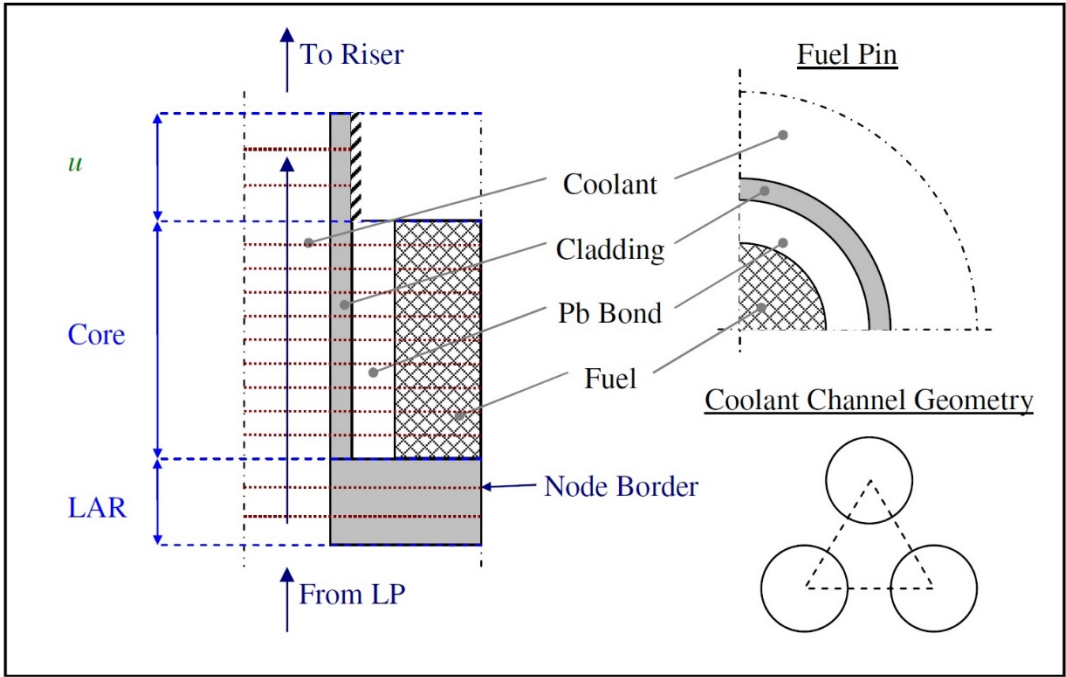


Figure 16. Core Structure, Geometry, and Nodes for the Plant Dynamics Code. Source [18].

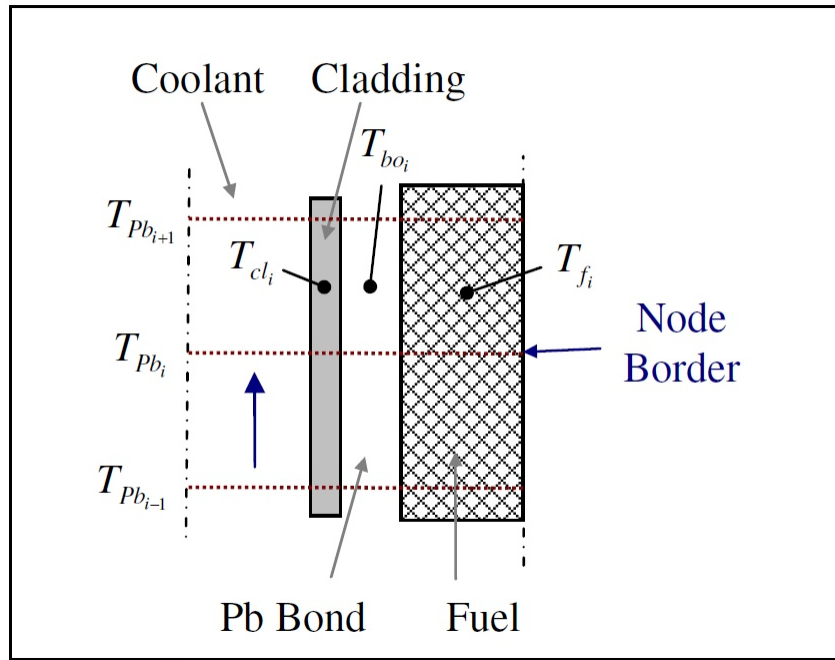


Figure 17. Nodes for Core Temperatures. Source [18].

While it understood that the setup shown in Figures 16 and 17 is not exactly the same for every liquid metal cooled fast reactor, the concept of liquid metal coolant flow interacting with cladding and a fuel region in a vertical loop is the most common setup and this very localized consideration can ignore the diversity of designs outside this region. This model also allows for coolant flow to be natural convection or pump driven as only the coolant flow rate is considered.

In order to calculate the rate of temperature change in the core, the change in enthalpy from the coolant flowing in and out of region i and the heat transfer from the cladding to coolant is required. The general equations to start with were [18]:

$$M_{coolant_i} \frac{\partial h}{\partial t} = \dot{m}_{coolant} [h_i - h_{i+1}] + Q_{cl,coolant_i} \quad (13)$$

$$Q_{cl,coolant_i} = \frac{T_{cl_i} - T_{coolant,avg}}{\frac{1}{HTC_i A_i} + (1/2) \frac{\ln\left(\frac{r_{cl,out}}{r_{cl,in}}\right) r_{cl,out}}{k_{cl_i} A_i}} \quad (14)$$

where M = mass of the coolant = $vol_i \times \rho_{coolant}$,

h = specific enthalpy,

\dot{m} = coolant flow rate,

in, out = values at cladding/fuel boundaries,

Q = heat transfer.

$HTC \propto \frac{k_{coolant_i}}{D_h}$ = coolant heat transfer coefficient,

$A = \pi d_{rod} \Delta x_i N_{rod}$ = heat transfer area,

k = thermal conductivity,

r = radius of cladding.

To simplify the heat transfer equation, the thermal resistances for the cladding and coolant are combined into one term [18]:

$$res_{coolant,cl_i} = \frac{1}{HTC_i \pi d_{rod}} + \frac{1}{2} \frac{\ln\left(\frac{r_{cl,out}}{r_{cl,in}}\right)}{2\pi k_{cl_i}} \quad (15)$$

$$Q_{cl,coolant_i} = \frac{\Delta x_i N_{rod}}{res_{coolant,cl_i}} \left(T_{cl_i} - \frac{T_{coolant_i} + T_{coolant_{i+1}}}{2} \right) \quad (16)$$

The values for the coolant properties (heat capacity, thermal conductivity, density, and viscosity) are obtained from the temperature dependent equations explained in Chapter III (equations 1–12). The cladding material is assumed to be HT-9 for each modeled design to ensure consistency, and the empirical equation for the thermal conductivity of HT-9 is [18]:

$$k_{cl} = 17.672 + 2.428^{-2} T - 1.696^{-5} T^2 \quad (17)$$

Finally, all the portions of the analysis are combined into one equation that gives the change in temperature for the coolant in the $i+1$ region as a function of time, with enthalpy being transformed into heat capacity and temperature terms [18]:

$$\frac{\partial T_{coolant_{i+1}}}{\partial t} = \frac{1}{M_{coolant_i}} \dot{m}_{coolant} (T_{coolant_i} - T_{coolant_{i+1}}) + \frac{\Delta x_i N_{rod}}{M_{coolant_i} c_{p,coolant_i} res_{coolant,cl_i}} \left(T_{cl_i} - \frac{T_{coolant_i} + T_{coolant_{i+1}}}{2} \right) \quad (18)$$

The mass of the coolant is derived each iteration from the core volume multiplied by the density of the coolant at the temperature of region i . Heat capacity and thermal conductivity (included in the coolant resistance heat transfer coefficient term HTC) are directly obtained from their respective coolant property equations for the current step temperature. Since each set of reactor designs gave a single ideal mass flow rate value (optimized for the related coolant type), the viscosity value for each coolant was multiplied by the $\dot{m}_{coolant}$ term to provide an input on temperature change from the different resistance-to-flow from each coolant. Actual flow could be adjusted for different coolants by changing coolant pump parameters (in a pump driven design), but this viscosity correction better simulates plant conditions for natural circulation designs and comparing coolant types.

C. MATLAB RESULTS

To compare the three coolants visually, (18) was graphed over the temperature range of 300 to 1100 K, with zoomed in views encompassing the normal operating ranges also presented. Most reactors are bound by a lower limit of 600 K due to the freezing point of lead and an upper limit of 900 K due to the onset of HT-9 cladding damage. The values for the y-axis (dT/dt) are unitless values only useful for comparing the different coolants and not true values for change in temperature in K over time. This is a result of some assumptions and modifications made to the heat transfer equations in order to model them separately from the full reactor code. Figures 18 and 19 show the rate of change of the coolant temperature for the three liquid metal coolants from the ARC-100 reactor design.

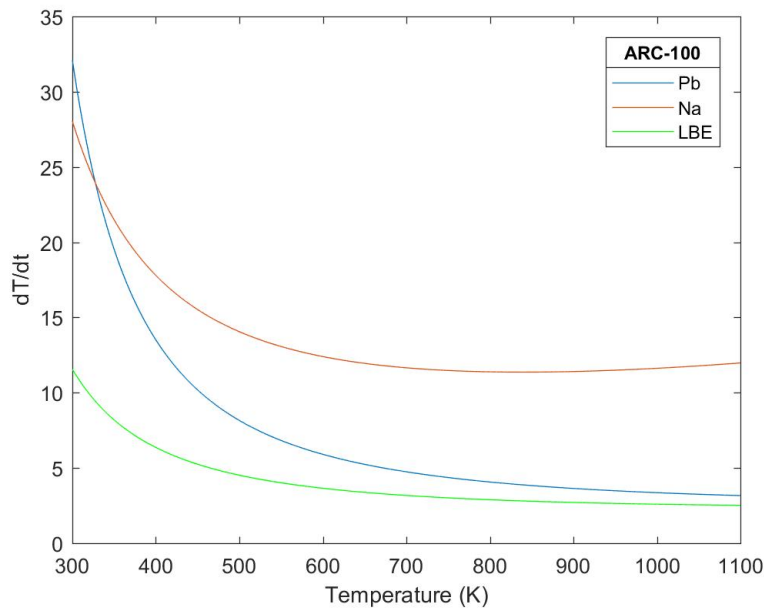


Figure 18. Temperature Change Rate for Three Coolants for ARC-100 Design.

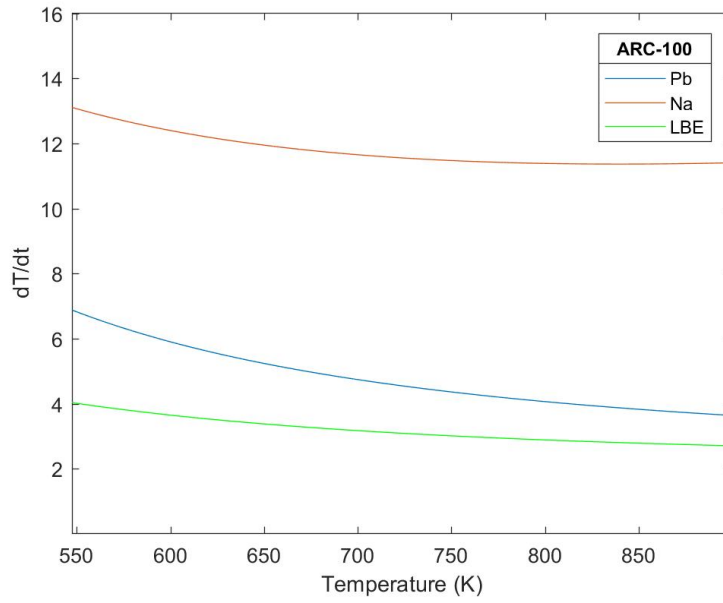


Figure 19. Zoomed Temperature Change Rate for Three Coolants for ARC-100 Design.

Figures 20 and 21 present the change in temperature rate at different coolant temperatures for the STAR-LM reactor design.

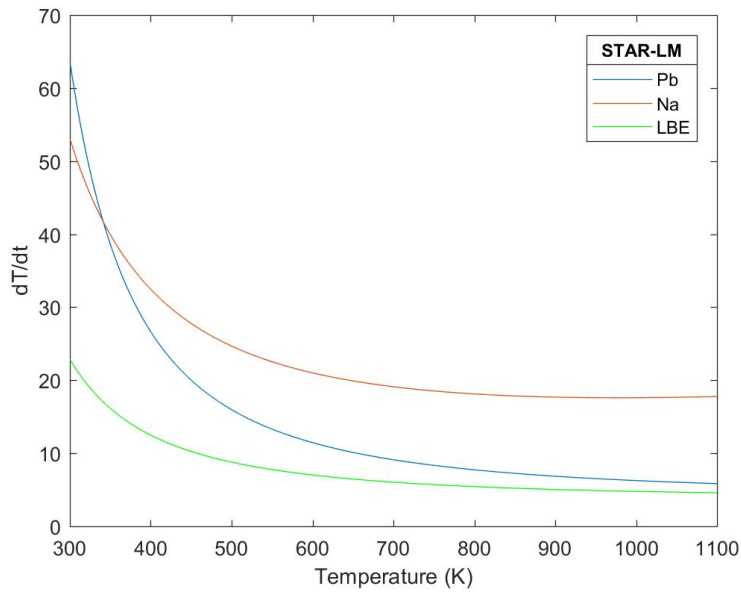


Figure 20. Temperature Change Rate for Three Coolants for STAR-LM Design.

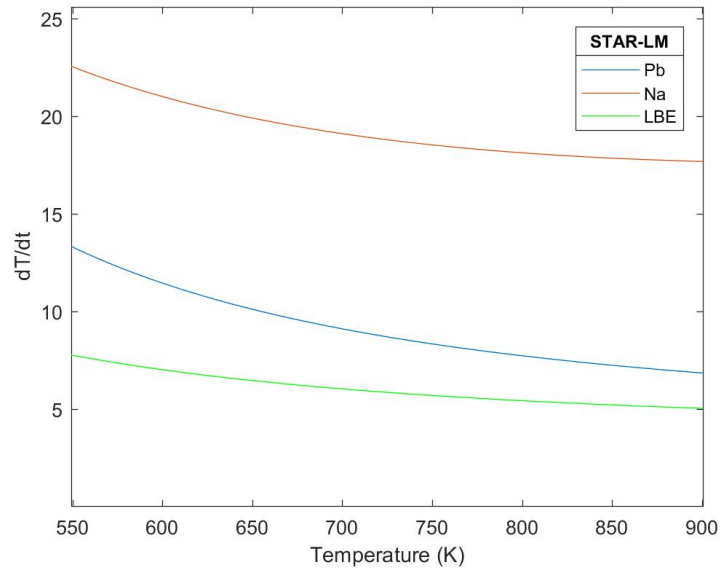


Figure 21. Zoomed Temperature Change Rate for Three Coolants for STAR-LM Design.

Figures 22 and 23 show the same equations graphed for the SVBR-75 design.

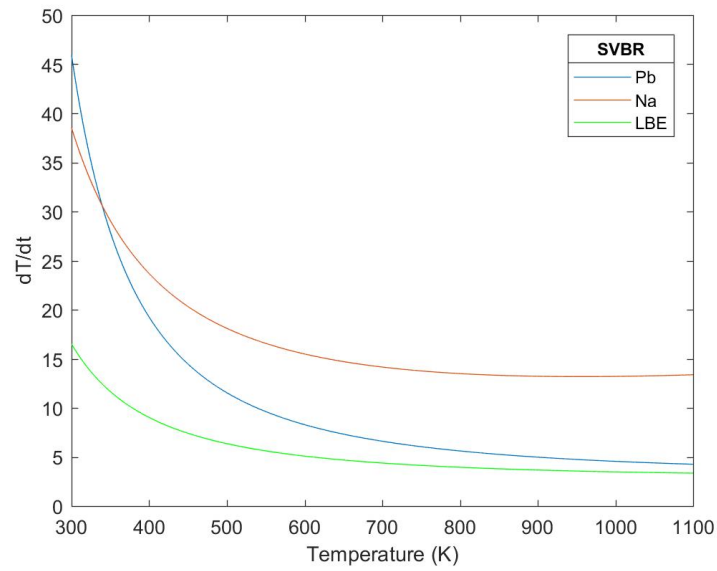


Figure 22. Temperature Change Rate for Three Coolants for SVBR-75 Design.

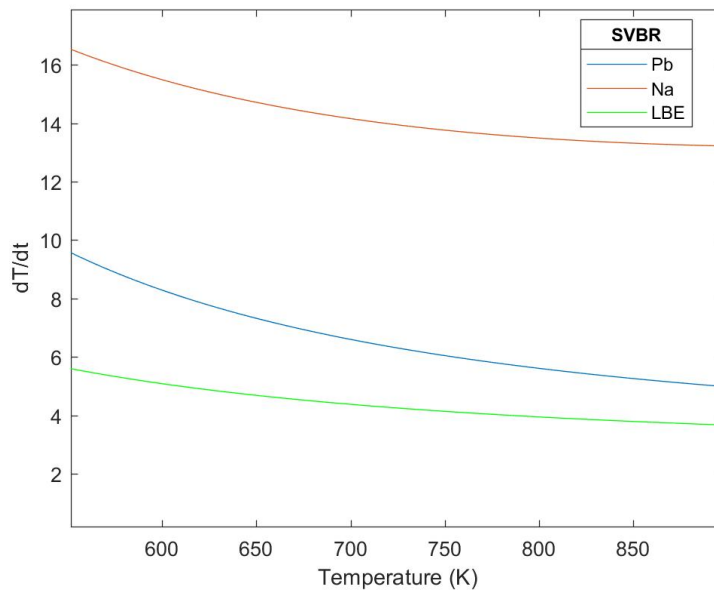


Figure 23. Zoomed Temperature Change Rate for Three Coolants for SVBR-75 Design.

To compare all three reactor designs and their three coolant options together, Figure 24 shows a composite of all three graphs into one.

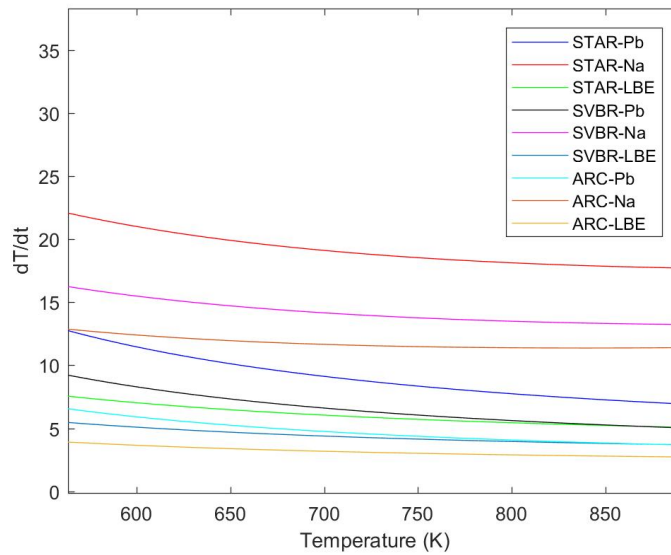


Figure 24. Change in Temperature Rate vs. Temperature for Three Reactor Designs.

In addition to graphing the rate of change in coolant temperature, a useful combination of density and neutron interactions for coolants was graphed as well. The elastic cross section was chosen because it is the largest and most desirable of the three main neutron interactions (RC, EL, NON). Individually Figures 4 and 13 show interesting properties of the three coolants but do not provide a good comparison tool. To make it more useful, this analysis took the density for each coolant at 700 K and determined how many atoms would be present per cubic centimeter of coolant using molecular weight and Avogadro’s number. Once this was determined, it was combined that with the elastic scattering cross sections for the fast energy spectrum to show the shifted cross section for elastic scattering per cubic centimeter of coolant. Table 4 summarizes the shift factor for each coolant that is applied to the elastic scattering cross section values.

Table 4. Atomic Density of Coolants

Coolant	Molecular Weight (g)	Density (g/cc) (at 700 K)	Atoms/cc	Shift Value
Lead (Pb-208)	208	10.545	3.053e22	.3053
Sodium (Na-23)	23	.85	2.226e22	.2226
LBE	208.45	10.16	2.935e22	.2935

From Table 4 it can be seen that sodium is most affected due to having the least number of atoms per cubic centimeter of coolant. This means that there are fewer atoms of sodium than lead or LBE available for elastic scattering in a given volume of coolant and therefore less ability to return neutrons to the fuel at fast energies. The shift value reflects this atomic density property by reducing the elastic scattering cross sections across the fast energy spectrum by the respective shift value to provide a more accurate representation of neutron interaction in a volume of coolant as compared to single atoms shown in Figure 13.

Figure 25 highlights the shifted elastic scattering cross sections of each coolant and Figure 26 shows the effect of the shift factor for each coolant.

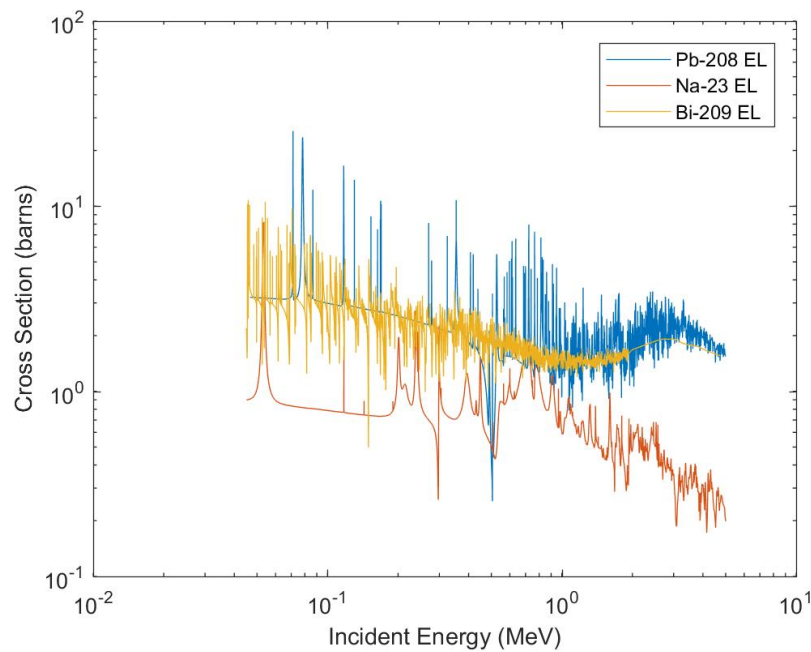


Figure 25. Shifted Elastic Scattering Cross Sections of Coolants. Adapted from [8].

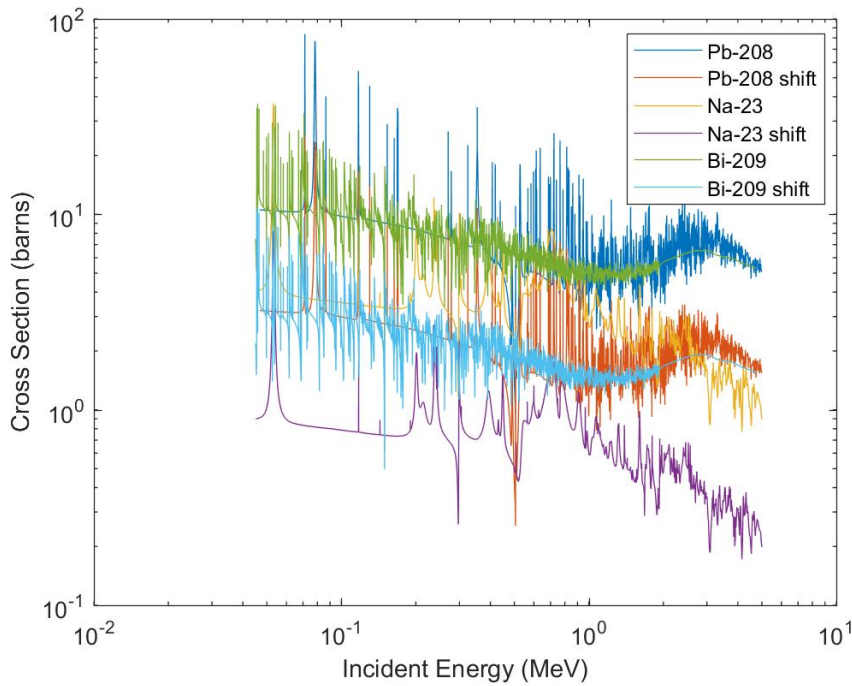


Figure 26. Shifted vs. Original Elastic Scattering Cross Sections of Coolants. Adapted from [8].

Figure 25 looks very much like Figure 13, with the same relative separation between sodium and lead and LBE above 1 MeV. Figure 26 shows how each cross section is shifted down by applying the coolant density, with slightly more separation between the sodium and other two coolants growing as the shift factor is applied.

D. ANALYSIS

1. Interpretations of dT/dt Graphs

From each set of graphs, it is evident that sodium has a clear advantage over lead and LBE with a higher rate of temperature change in the operating band for each reactor design. Even the lowest dT/dt rate for sodium coolant (ARC-100) is above the highest rate for the lead cooled (STAR-LM) and LBE cooled (SVBR-75) designs. Somewhat unsurprisingly the highest curves for lead and LBE coolants relate to the reactor designs that were optimized for that coolant type. It is interesting to note that the sodium coolant-based design (ARC-100) reflects the lowest values of the three sodium curves. These

results indicate that the thermal conductivity and viscosity of a coolant have greater impact than the density and heat capacity on the change in temperature rate since sodium had a more desirable profile than lead or LBE for these physical properties. Additionally, while there are some small, introduced errors from assumptions and simplifying reactor designs to fit the model equations, these are consistent for all three coolants. This results in sodium showing a nearly 100% advantage over lead and almost 200% increase over LBE for the 550 to 900 K temperature range. This shows that it is possible to compare reactor designs based on the rate of change in coolant temperature for different coolants with clear separation between the coolant curves. In this respect, sodium (Na-23 specifically) is the best coolant type for having rapid coolant temperature response to power changes.

2. Reactivity Considerations

The second part of determining a successful comparison between the coolants is looking at their neutron interactions and reactivity addition rates. The larger the reactivity coefficient, the more the coolant affects power changes and load following capability. Typically, coolant temperature serves as a correction factor to power change, with the higher temperature that results from increased power demand curbing the power spike through the negative temperature coefficient of reactivity. Table 3 showed a sample of temperature coefficients of reactivity for selected coolants, with most being negative as desired by the GEN IV goals [1]. However, the Integral Fast Reactor (IFR) design had a positive temperature coefficient while the LBE based design was slightly positive but closer to zero at normal operating temperatures. This shows the difficulty in comparing coolants and designs because the core geometry has such an impact on the reactivity coefficient value and sign. A larger core will tend towards a negative effect on reactivity as temperature increases due to the larger impact of neutron leakage from increased migration length while smaller cores will see a harder neutron spectrum and positive reactivity impact [23]. As such, it is not possible to compare non-identical reactor designs for the purpose of choosing the best coolant for ALF based on reported reactivity values alone.

What is shown in Table 4 and Figure 26 is that the neutronic and physical properties of coolants can be coupled and compared for different core temperature conditions. While the density values for Table 4 were based on a coolant temperature of 700 K, additional tables and graphs at reactor design specific inlet/outlet temperatures can be calculated and easily attached to the neutron interaction data of interest to provide comparison tools for the considered design. Further analysis of Figures 8–10 show that lead and sodium have the greater separation between neutron “gaining” interactions (elastic scattering) and neutron “loss” interactions (inelastic scattering and radiative capture). Lead has the greatest separation, averaging five orders of magnitude between gain and loss interactions, while sodium has a similar separation for elastic scattering and radiative capture, but much less separation for inelastic scattering. This smaller inelastic scattering separation is difficult to qualitatively compare because a neutron may or may not remain in the fast spectrum after an inelastic scattering event, with the probability beyond the scope of data available in Figure 9. Figure 11 very clearly shows that bismuth has the smallest gain vs. loss separation, only 2–3 orders of magnitude, making it the least desirable in terms of returning neutrons to the core in a fast state. Finally, Figures 12 and 14 along with Figure 25 highlight the advantage of lead over sodium in an overall comparison, with the higher elastic scattering and much lower inelastic scattering cross sections overwhelming the slight radiative capture cross section disadvantage. Analysis of these graphs also concludes that lead is superior to LBE based on the poor performance of bismuth in the available elastic scattering and radiative capture cross section data. This result supports the data in Table 3 that showed that lead cooled reactors had the largest magnitude temperature coefficient of reactivity of the reported reactor designs.

V. SUMMARY

Multiple conclusions can be made from the research presented in this thesis. The first is that answers for each question asked in the introduction were successfully obtained. Several physical properties and neutron interactions were identified that relate strongly to heat transfer and autonomous load following, with their impacts and zones of desirability investigated. Additionally, it is possible through plotting the shifted neutron interactions and heat transfer equations to provide a comparative analysis of the three considered liquid metal coolants and identify clear separation in the results to support choosing a specific liquid metal coolant, with sodium being the “winner” in this comparison.

The second conclusion is that the neutronic interaction and the rate of coolant temperature change results provide contradicting “winners” for coolant selection based on the considered properties. The rate of temperature change for sodium was consistently nearly double that of lead and LBE, but lead had a steady margin of advantage for elastic scattering over sodium. Complicating comparison was the fact that there is no simple method to translate neutron interaction for each coolant into temperature coefficients of reactivity in a specific reactor design without a full and design specific reactor code, as seen by the varied results in Table 3. My conclusion is that the advantage of sodium regarding changing coolant temperature outweighs the natural advantage lead has in regard to neutron interaction. One way to close the heat transfer equation gap in lead’s favor would be to eliminate the viscosity disparity by utilizing coolant pumps to neutralize the first terms in equation (18) and adjust core geometry to favor lead’s better elastic scattering properties.

The final conclusion is that there is significant research still to be done in many areas of liquid metal coolants and autonomous load following. This thesis was valuable in showing that coolant comparison is both useful and possible, but the results still leave room for contrasting interpretation by supporters of both lead and sodium coolant technology. This comparative analysis of coolants could be improved with a broader range of coolant reactivity values to compare, more reactor design details to model, and a computer code that is built to uncouple equation (18) from a larger model, refining the heat transfer rate

graphs, and incorporating the neutron interactions to remove the user interpretation of the ENDF graphs.

An area of additional research is comparing autonomous load following through passive reactivity change to base load reactors with energy storage (thermal, hydroelectric, or batteries) in response to power transients. The idea of heat storage as a method of load following is more applicable for larger reactor plants, especially commercial and large surface ships, that have the physical space for large water tanks and piping. Most submarines already have a method of battery energy storage for emergency operations, siphoning off a small trickle of power during reactor operation to maintain full charge. Future research could be conducted into the economic comparison of ALF versus energy storage and power transient response time and fuel burnup.

One finding in this thesis was that no ENDF data exists for LBE and is limited for Bismuth-209. With the use of LBE as a fast reactor coolant a legitimate option being considered, detailed neutron interaction data would be vital for modeling LBE cooled reactors and more fairly comparing LBE coolant to other liquid metals instead of using Bi-209 as a stand in. Future work should be conducted to expand the ENDF to include LBE and refined for all liquid metals in the fast spectrum to ensure maximum accuracy.

It should be noted that while this thesis concluded that sodium was the superior liquid metal coolant for ALF based on neutron interactions and reactivity addition from the rate of heat transfer, autonomous load following is not the only consideration when selecting a reactor coolant. Each of the three considered coolants have significant non-reactivity concerns, with sodium's explosive interaction with water and lead and LBE's high corrosivity providing considerable design and safety concerns. Any future reactor design needs to take into account the full range of coolant properties and this research and comparison of temperature-based reactivity addition is simply one aspect of that consideration. Considerable research is already being conducted, comparing liquid metal coolants to provide design input criteria, with tables produced by Levent Can highlighting an example of this process [13]. Additionally, cost and availability of materials was not considered in this thesis but would be a necessary part of any real-world economic study for a reactor design when choosing the coolant type.

LIST OF REFERENCES

- [1] J. Kelly, “Atoms for Peace – The Next Generation,” GEN-4, September 29, 2016. [Online]. Available: https://www.gen-4.org/gif/jcms/c_84314/webinar-series-1-atoms-for-peace-the-next-generation
- [2] “List of Nuclear Reactors,” *Wikipedia*. Accessed September 8, 2018. [Online]. Available: https://en.wikipedia.org/wiki/List_of_nuclear_reactors
- [3] B. Hill, “Sodium Cooled Fast Reactors,” GEN-4, November 22, 2016. [Online]. Available: https://www.gen-4.org/gif/jcms/c_87283/webinar-series-4-sodium-cooled-fast-reactors
- [4] C. Smith, “Lead Fast Reactor (LFR),” GEN-4, June 12, 2017. [Online]. Available: https://www.gen-4.org/gif/jcms/c_92385/craigsmith-gif-webinarannouncement-22-may-2017
- [5] “Lead-cooled fast reactor,” *Wikipedia*. Accessed August 26, 2018. [Online]. Available: https://en.wikipedia.org/wiki/Lead-cooled_fast_reactor
- [6] “Sodium-cooled fast reactor,” *Wikipedia*. Accessed August 26, 2018. [Online]. Available: https://en.wikipedia.org/wiki/Sodium-cooled_fast_reactor
- [7] V. Sobolev, “Database of thermophysical properties of liquid metal coolants for GEN-IV,” SCK CEN Belgian Nuc. Res. Centre, Mol, Belgium, Rep. 1069, 2011.
- [8] International Atomic Energy Agency, “Evaluated Nuclear Data File (ENDF),” April 20, 2018. [Online]. Available: <https://www-nds.iaea.org/exfor/endl.htm>
- [9] A. Moiseyev and J. J. Sienicki. “Development of a Plant Dynamics Computer Code for Analysis of a Supercritical Carbon Dioxide Brayton Cycle Energy Converter Coupled to a Natural Circulation Lead-Cooled Fast Reactor,” Arg. Nat’l Lab, Argonne, IL, Rep. 06–27, 2006.
- [10] D. J. Watts, “Isotope mixes, corresponding nuclear properties and reactor design implications of naturally occurring lead sources,” M.S. thesis, Dept. of Physics, NPS, Monterey, CA, USA, 2013. [Online]. Available: <http://hdl.handle.net/10945/34758>
- [11] *Nuclear Physics Chapter NP-5: Nuclear Reactions*, BHI Energy, Benton Harbor, MI, USA, 2005. [Online]. Available: <https://www.bhienergy.com/employee-resources/training/NP-5.pdf>
- [12] *DOE Fundamentals Handbook Nuclear Physics and Reactor Theory Volume 2 of 2*, Dept. of Energy, Washington, DC, USA, 1993. [Online]. Available: <http://large.stanford.edu/courses/2013/ph241/waisberg1/docs/h1019v2.pdf>

- [13] L. Can, “Analysis of coolant options for advanced metal cooled nuclear reactors,” M.S. thesis, Dept. of Physics, NPS, Monterey, CA, USA, 2006. [Online]. Available: <http://hdl.handle.net/10945/2379>
- [14] T. Sathiyasheela, G. S. Srinivsaan, K. Devan, and S. C. Chetal, “Methodology to Enhance Negative Reactivity,” presented at IAEA Tech. Mtg. on Fast Reactor Designs, Vienna, Austria, Feb. 27, 2012.
- [15] S. L. Svanstrom, “Load following with a passive reactor core using the SPARC design,” M.S. thesis, Dept. of Applied Nuclear Physics, Uppsala Universitet, Uppsala, Sweden, 2016.
- [16] Nuclear Energy Agency, “Technical and Economic Aspects of Load Following with Nuclear Power Plants,” Washington, DC, USA, 2011.
- [17] M. A. Shahzad, L. Qin, and S. S. Imam, “Analysis of lead-cooled fast reactor using a core simulator,” *Progress in Nuclear Energy*, vol. 104, pp. 229–241, Apr. 2018 [Online]. <https://doi.org/10.1016/j.pucene.2017.10.002>
- [18] A. Moiseyev and J. Sienicki, “ANL Plant Dynamics Code and Control Strategy Development for the Supercritical Carbon Dioxide Brayton Cycle,” in *Proceedings of SCCO2 Pwr. Cycle Symp.*, Troy, NY, 2009.
- [19] J. J. Sienicki and P. V. Petkov, “Autonomous Load Following and Operational Aspects of the Star-LM HLMC Natural Convection Reactor,” in *Proceedings of ICONE 10: Tenth Int’l Conf. on Nuc. Eng.*, Arlington, VA, 2002.
- [20] P. E. MacDonald and J. Buongiorno, “Design of an Actinide Burning, Lead or Lead-Bismuth Cooled Reactor That Produces Low Cost Electricity,” Idaho Nat’l Eng. and Env. Lab Bechtel, Idaho, USA, Rep-092, 2002.
- [21] D. Wade, “ARC-100 Introduction,” presented at MEV Summer School, Argonne, Illinois, USA, July 18, 2018.
- [22] IAEA, “Liquid Metal Coolants for Fast Reactors Cooled by Sodium, Lead, and Lead-Bismuth Eutectic,” Vienna, Austria, Rep. NP-T-1.6, 2012.
- [23] “Energy Transport,” class notes for MIT22-05: Neutron Science and Reactor Physics, Dept. of Physics, MIT, Cambridge, MA, fall 2009. [Online]. Available: https://ocw.mit.edu/courses/nuclear-engineering/22-05-neutron-science-and-reactor-physics-fall-2009/lecture-notes/MIT22_05F09_lec08-09.pdf

INITIAL DISTRIBUTION LIST

1. Defense Technical Information Center
Ft. Belvoir, Virginia
2. Dudley Knox Library
Naval Postgraduate School
Monterey, California